elastography for the detection of complications in patients with cirrhosis. Liver Int. 2012;32:852–8.
35. Bota S, Sporea I, Sirli R, et al. Can ARFI elastography predict the presence of significant esophageal varices in newly diagnosed cirrhotic patients? Ann Hepatol. 2012;11:519–25.
36. Takuma Y, Nouso K, Morimoto Y, et al. Measurement of spleen stiffness by acoustic radiation force impulse imaging identifies cirrhotic patients with esophageal varices. Gastroenterology. 2012;144:92–101.
37. Castera L, Le Bail B, Roudot-Thoraval F, et al. Early detection in routine clinical practice of cirrhosis and oesophageal varices in chronic hepatitis C: comparison of transient elastography (FibroScan) with standard laboratory tests and non-invasive scores. J Hepatol. 2009;50:59–68.

OPEN ACCESS Freely available online

PLOS | ONE

Induction of Cell-Mediated Immune Responses in Mice by DNA Vaccines That Express Hepatitis C Virus NS3 Mutants Lacking Serine Protease and NTPase/RNA Helicase Activities

Suratno Lulut Ratnoglik[1,3], Da-Peng Jiang[1], Chie Aoki[1,2], Pratiwi Sudarmono[3], Ikuo Shoji[1], Lin Deng[1], Hak Hotta[1]*

1 Division of Microbiology, Kobe University Graduate School of Medicine, Kobe, Japan, **2** JST/JICA SATREPS Laboratory of Kobe University, Faculty of Medicine, University of Indonesia, Jakarta, Indonesia, **3** Faculty of Medicine, University of Indonesia, Jakarta, Indonesia

Abstract

Effective therapeutic vaccines against virus infection must induce sufficient levels of cell-mediated immune responses against the target viral epitopes and also must avoid concomitant risk factors, such as potential carcinogenic properties. The nonstructural protein 3 (NS3) of hepatitis C virus (HCV) carries a variety of $CD4^+$ and $CD8^+$ T cell epitopes, and induces strong HCV-specific T cell responses, which are correlated with viral clearance and resolution of acute HCV infection. On the other hand, NS3 possesses serine protease and nucleoside triphosphatase (NTPase)/RNA helicase activities, which not only play important roles in viral life cycle but also concomitantly interfere with host defense mechanisms by deregulating normal cellular functions. In this study, we constructed a series of DNA vaccines that express NS3 of HCV. To avoid the potential harm of NS3, we introduced mutations to the catalytic triad of the serine protease (H57A, D81A and S139A) and the NTPase/RNA helicase domain (K210N, F444A, R461Q and W501A) to eliminate the enzymatic activities. Immunization of BALB/c mice with each of the DNA vaccine candidates (pNS3[S139A/K210N], pNS3[S139A/F444A], pNS3[S139A/R461Q] and pNS3[S139A/W501A]) that expresses an NS3 mutant lacking both serine protease and NTPase/helicase activities induced T cell immune responses to the degree comparable to that induced by the wild type NS3 and the NS3/4A complex, as demonstrated by interferon-γ production and cytotoxic T lymphocytes activities against NS3. The present study has demonstrated that plasmids expressing NS3 mutants, NS3(S139A/K210N), NS3(S139A/F444A), NS3(S139A/R461Q) and NS3(S139A/W501A), which lack both serine protease and NTPase/RNA helicase activities, would be good candidates for safe and efficient therapeutic DNA vaccines against HCV infection.

Citation: Ratnoglik SL, Jiang D-P, Aoki C, Sudarmono P, Shoji I, et al. (2014) Induction of Cell-Mediated Immune Responses in Mice by DNA Vaccines That Express Hepatitis C Virus NS3 Mutants Lacking Serine Protease and NTPase/RNA Helicase Activities. PLoS ONE 9(6): e98877. doi:10.1371/journal.pone.0098877

Editor: Golo Ahlenstiel, University of Sydney, Australia

Received September 29, 2013; **Accepted** May 7, 2014; **Published** June 5, 2014

Funding: This study was supported in part by a SATREPS Grant from Japan Science and Technology Agency (JST) and Japan International Cooperation Agency (JICA), a grant from the Japan Initiative for Global Research Network on Infectious Diseases (J-GRID), Ministry of Education, Culture, Sports, Science and Technology, Japan, and the Health and Labour Sciences Research Grants from the Ministry of Health, Labour and Welfare, Japan. This study was also carried out as part of the Global Center of Excellence (G-COE) Program at Kobe University Graduate School of Medicine. The funders had no role in study design, data collection and analysis, decision to publish, or preparation of the manuscript.

Competing Interests: The authors have declared that no competing interests exist.

* E-mail: hotta@kobe-u.ac.jp

Introduction

Hepatitis C virus (HCV) is an enveloped RNA virus that belongs to the genus *Hepacivirus* of the family *Flaviviridae*. The viral genome encodes a single polyprotein of about 3,000 amino acids, which is cleaved by host and viral proteases to generate at least 10 viral proteins, i.e., envelope 1 (E1) and E2, p7, nonstructural protein 2 (NS2), NS3, NS4A, NS4B, NS5A and NS5B. NS3 is a multi-functional protein with a serine protease domain located in the N-terminal one-third and a nucleoside triphosphatase (NTPase)/RNA helicase domain located in the C terminal two-thirds, which are involved in the proteolytic processing of the viral polyprotein and viral RNA replication, respectively [1,2,3].

HCV is a major cause of chronic liver disease, such as chronic hepatitis, liver cirrhosis and hepatocellular carcinoma. It is estimated that 180 million people are currently infected with HCV worldwide, and that ca. 70% of them become chronically infected [4,5]. The recent approval of NS3 serine protease inhibitors for treatment of HCV genotype 1 infection was a great progress in HCV antiviral development, and combination of a protease inhibitor with interferon (IFN) and ribavirin has increased sustained virological response (SVR) in patients [6]. On the contrary, great success has not been achieved in HCV vaccine development; no effective HCV vaccine is available so far, either for a prophylactic or a therapeutic purpose.

While prophylactic HCV vaccines must have capacity to induce protective levels of neutralizing antibodies directed principally to the viral protein E2, effective therapeutic HCV vaccines must elicit strong cell-mediated immune responses against a wide variety of $CD4^+$ and $CD8^+$ epitopes of the viral origin. NS3 is known to carry a variety of $CD4^+$ and $CD8^+$ T cell epitopes to induce strong HCV-specific T cell responses, which are correlated with viral

clearance and resolution of acute HCV infection [7,8,9,10,11]. Also, the HCV core protein is known to carry a variety of $CD4^+$ and $CD8^+$ epitopes [7,8,9,12,13,14]. From the antigenic point of view, therefore, NS3 and the core protein would be attractive candidates to be used for therapeutic vaccines that elicit T cell-mediated immune responses against HCV.

Another important aspect to be assessed carefully in vaccine development is a potential risk(s) of the vaccine-derived peptides/proteins of the viral origin, which might impair or deregulate the normal functions of the host cells. For example, the HCV core protein is known to exhibit oncogenic properties in cell culture systems and transgenic mouse models [15,16,17]. The NS3 serine protease cleaves the mitochondrial antiviral signaling protein MAVS (also referred to as IPS-1, VISA and Cardif) to blockade the RIG-I- and TLR3/TRIF-mediated signaling for the induction of IFN-β production [3,18,19,20,21]. Also, NS3 inactivates T cell protein tyrosine phosphatase and modulates epithelial growth factor (EGF) signaling [22]. Moreover, the NS3 NTPase/RNA helicase, which is principally required for HCV RNA replication [1,2], may concomitantly deregulate cellular RNA helicase-mediated functions, such as DNA replication, RNA transcription, splicing, RNA transport, ribosome biogenesis, mRNA translation, RNA storage and decay [3,23,24,25]. These observations imply the possible involvement of NS3 in the development of hepatocellular carcinoma. Therefore, a vaccine expressing the functionally active core protein or NS3 may be disadvantageous to the vaccinees. To avoid those potential risks, we introduced a variety of point mutations that abolish the serine protease and NTPase/RNA helicase activities of NS3. We report here that a DNA vaccine that expresses an NS3 mutant lacking both serine protease and NTPase/RNA helicase activities induced strong cell-mediated immune responses in mice, with a high level of IFN-γ production and strong cytotoxic T lymphocyte (CTL) activities.

Materials and Methods

Plasmid Construction

Plasmids expressing the entire sequences of wild type NS3 (pSG5-NS3wt) and the NS3/4A complex (pSG5-NS3/4A) of the HCV MKC1a strain (genotype 1b) were derived from the previously reported ones, pcDNA3.1/NS3F(MKC1a) [26] and pcDNA3.1/MKC1a/4A [27], respectively, with the Myc-His tag deleted, and subcloned into the pSG5 vector (Stratagene, USA). To express a polyprotein consisting of full-length NS5A and C-terminally truncated NS5B (NS5A/5BΔC) as a substrate for the NS3 serine protease, the corresponding region of pTM1-NS5A/5BΔC [27] were subcloned into the pSG5 expression vector (Stratagene). Plasmids for production of glutathione S-transferase (GST) and GST-fused NS3 (GST-NS3) were also described previously [26]. An NS3 expression plasmid in the backbone of pEF1/Neomycin(+) (Invitrogen, NY), pEF1/Neo-NS3, was constructed. pIFNβ-Luc, which contains firefly luciferase reporter gene under the control of the interferon β promoter, was a kind gift from Dr. T. Fujita (Kyoto University, Kyoto, Japan) [28]. pRL-TK (Promega), which expresses Renilla luciferase, was used as an internal control. To express an N-terminal part of retinoic acid-inducible gene I (N-RIG-I) [28], the corresponding genomic region was amplified by RT-PCR from Huh-7 cellular RNA and subcloned into an expression vector to generate pEF1A/N-RIG-I-FLAG. pSG5-NS4A was described previously [27].

Single-point mutations were introduced by site-directed mutagenesis into each of the catalytic triad of the NS3 serine protease [29,30,31,32,33] to generate pNS3(H57A), pNS3(D81A) and pNS3(S139A) that express NS3 mutants lacking the serine protease activity (Fig. 1). Additional mutations, which have been reported to abolish the NTPase/RNA helicase activities of NS3 [34,35,36], were introduced into pNS3(S139A) to generate pNS3(S139A/K210N), pNS3(S139A/F444A), pNS3(S139A/R461Q) and pNS3(S139A/W501A). The primers used for the site-directed mutagenesis are shown in Table 1. Introduction of proper mutations were verified by DNA sequencing.

Cells and Protein Expression

The human hepatoma cell line Huh-7.5 [37] was kindly provided by Dr. Charles M. Rice (The Rockefeller University, New York, NY, USA). Huh-7 and Huh-7.5 cells were cultured in Dulbecco's modified Eagle's medium (DMEM) (high glucose) supplemented with 2 mM L-glutamine, 0.1 mM non-essential amino acids (Invitrogen), 50 IU/ml penicillin, 50 μg/ml streptomycin and 10% heat-inactivated fetal calf serum (FCS; Biowest,

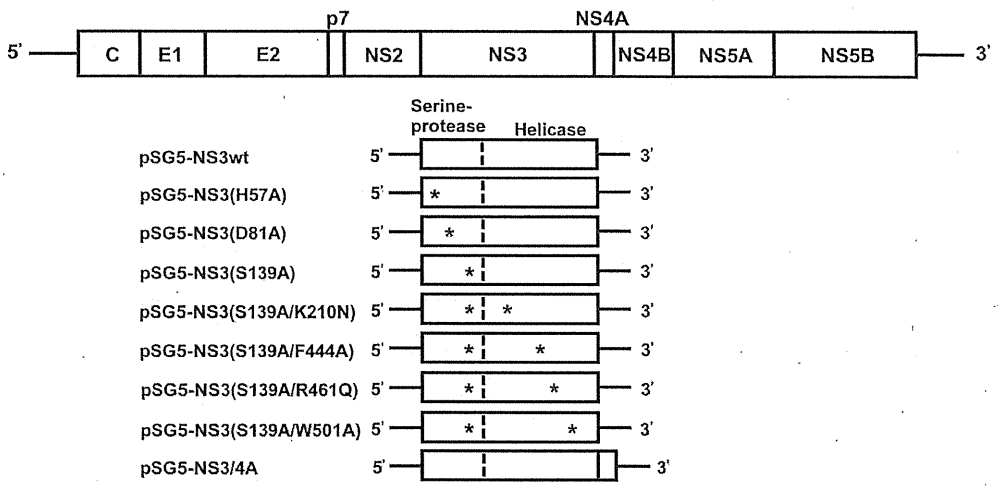

Figure 1. Schematic representation of the HCV genome and the NS3 region with various point mutations. The HCV genome (top) as well as NS3wt and various NS3 mutants are shown. Asterisks indicate point mutations in the serine protease and NTPase/RNA helicase domains.
doi:10.1371/journal.pone.0098877.g001

Table 1. Primers used for the introduction of HCV NS3 mutations.

NS3 mutation	Position	Sequence*	Direction
H57A	nt 154 to 182	5′-TGTTGGACTGTCTATGCTGGTGCCGGCTC-3′	Forward
		5′-GAGCCGGCACCAGCATAGACAGTCCAACA-3′	Reverse
D81A	nt 229 to 258	5′-AATGTAGACCAAGCCCTCGTTGGCTGGCCG-3′	Forward
		5′-CGGCCAGCCAACGAGGGCTTGGTCTACATT-3′	Reverse
S139A	nt 401 to 430	5′-ACCTGAAGGGTTCCGCGGGTGGTCCGCTGC-3′	Forward
		5′-GCAGCGGACCACCCGCGGAACCCTTCAGGT-3′	Reverse
K210A	nt 616 to 647	5′-ACTGGCAGCGGCAACAGCACCAAGGTGCCGGC-3′	Forward
		5′-GCCGGCACCTTGGTGCTGTTGCCGCTGCCAGT-3′	Reverse
F444A	nt 1315 to 1347	5′-AGCTTGGACCCTACTGCCACCATCGAGACGACG-3′	Forward
		5′-CGTCGTCTCGATGGTGGCAGTAGGGTCCAAGCT-3′	Reverse
R461Q	nt 1369 to 1401	5′-TCGCGCTCGCAGCAGCGAGGCAGGACTGGTAGG-3′	Forward
		5′-CCTACCAGTCCTGCCTCGCTGCTGCGAGCGCGA-3′	Reverse
W501A	nt 1484 to 1517	5′-ATGACGCGGGCTGTGCTGCGTACGAGCTCACGCC-3′	Forward
		5′-GGCGTGAGCTCGTACGCAGCACAGCCCGCGTCAT-3′	Reverse

*The mutated residues in the primer sequences are underlined; nt, nucleotide.

doi:10.1371/journal.pone.0098877.t001

France) at 37°C in a 5% CO_2 incubator. For ectopic protein expression, Huh-7.5 cells were transfected with the respective plasmids using X-tremeGENE 9 DNA Transfection Reagent (Roche, Mannheim, Germany) and cultured for 24 to 48 h. Protein expression was confirmed by immunoblotting and indirect immunofluorescence analyses using specific antibodies, as described previously [38].

P815 mouse lymphoblast-like mastocytoma cells (H-2^d) cultured in the complete DMEM were transfected with pEF1/Neo-NS3 and stable transfectants expressing NS3 were selected using neomycin (G418) (Nacalai Tesque, Kyoto, Japan). The NS3-expressing P815 cells were treated with 25 μg/ml of mitomycin C (Sigma-Aldrich, St. Louis, MO, USA) for 30 min (P815-NS3) and used as stimulator and target cells in a CTL assay using splenocytes obtained from NS3-immunized BALB/c mice (H-2^d), as described below.

GST-NS3 and GST were produced in *Escherichia coli* BL21 strain and purified with glutathione sepharose 4B beads (GE Healthcare, Buckinghamshire, UK). The proteins were eluted by reduced glutathione in a buffer containing 50 mM Tris-HCl (pH 8.0). After dialysis, the eluted protein was stored at −80°C until being used. The concentrations of purified proteins were determined using Pierce BCA Protein Assay Kit (Thermo Fisher Scientific Inc., Rockford, IL, USA).

Indirect Immunofluorescence

Cells seeded on glass coverslips in a 24-well plate were fixed with 4% paraformaldehyde in phosphate-buffered saline (PBS) for 15 min at room temperature and permeabilized with 0.1% Triton X-100 in PBS for 15 min at room temperature. After being washed with PBS twice, the cells were consecutively incubated with primary and secondary antibodies. The primary antibodies used were mouse monoclonal antibodies against NS3 (4A-3, a kind gift from Dr. I. Fuke, Research Foundation for Microbial Diseases, Osaka University, Kagawa, Japan) [27]. The secondary antibody used was Alexa Fluor 488-conjugated goat anti-mouse IgG (H+L) (Molecular Probes, Eugene, OR, USA). The stained cells were observed under an All-in-One fluorescence microscope (BZ-9000 Series, Keyence Corporation).

Immunoblotting

Cells were lysed with SDS sample buffer. Equal amounts of cell lysates were separated by 10% SDS-polyacrylamide gel electrophoresis and transferred onto a polyvinylidene difluoride membrane (Millipore, Bedford, MA, USA), which was then incubated with the respective primary antibodies, followed by incubation with peroxidase-conjugated secondary antibody. The primary antibodies used were mouse monoclonal antibodies against NS3, NS5A and GAPDH (Chemicon International, Temecula, CA, USA). The respective proteins were visualized using ECL immunoblotting detection reagents (GE Healthcare).

NS3 Serine Protease Assay

Huh-7.5 cells were co-transfected with two plasmids, one expressing NS3 and the other expressing an NS5A/NS5BΔC polyprotein as a substrate, and cultured for 24 h. The cells were lysed and the lysates were subjected to immunoblot analysis using anti-NS5A monoclonal antibody. NS3 serine protease activities were assessed by the cleavage of the NS5A/NS5BΔC polyprotein and emergence of the cleaved-off NS5A [27].

NS3 Helicase Assay

NS3 helicase activities were determined as described previously with some modifications [39,40]. In brief, a pair of DNA oligonucleotides (5′-biotin-GCTGACCCTGCTCCCAATCG-TAATCTATAGTGTCACCTA-3′ and 5′-digoxygenin-CGATTGGGAGCAGGGTCAGC-3′) were purchased (Operon Biotechnologies K.K., Tokyo, Japan). They were mixed at a 1:1 molar ratio and annealed to generate a DNA duplex substrate in 50 mM NaCl, 2 mM HEPES, 0.1 mM EDTA and 0.01% SDS by heating at 100°C for 5 min, followed by incubation at 65°C for 30 min and an annealing step at 22°C for 4 h. The DNA duplex substrate (2.5 ng/well) was immobilized via the biotin molecule on the surface of a NeutrAvidin Coated plate (Clear, 8-well strip; Thermo Fisher Scientific Inc.). A reaction mixture (90 μl) containin 11 nM of purified GST-NS3 [26], GST-NS3(K210N) or GST, 25 mM 4-morpholine-propanesulfonic acid (MOPS; pH 7.0), 5 mM ATP, 2 mM DTT, 3 mM $MnCl_2$ and 100 μg/ml of bovine serum albumin (BSA) was added to each well. Reactions

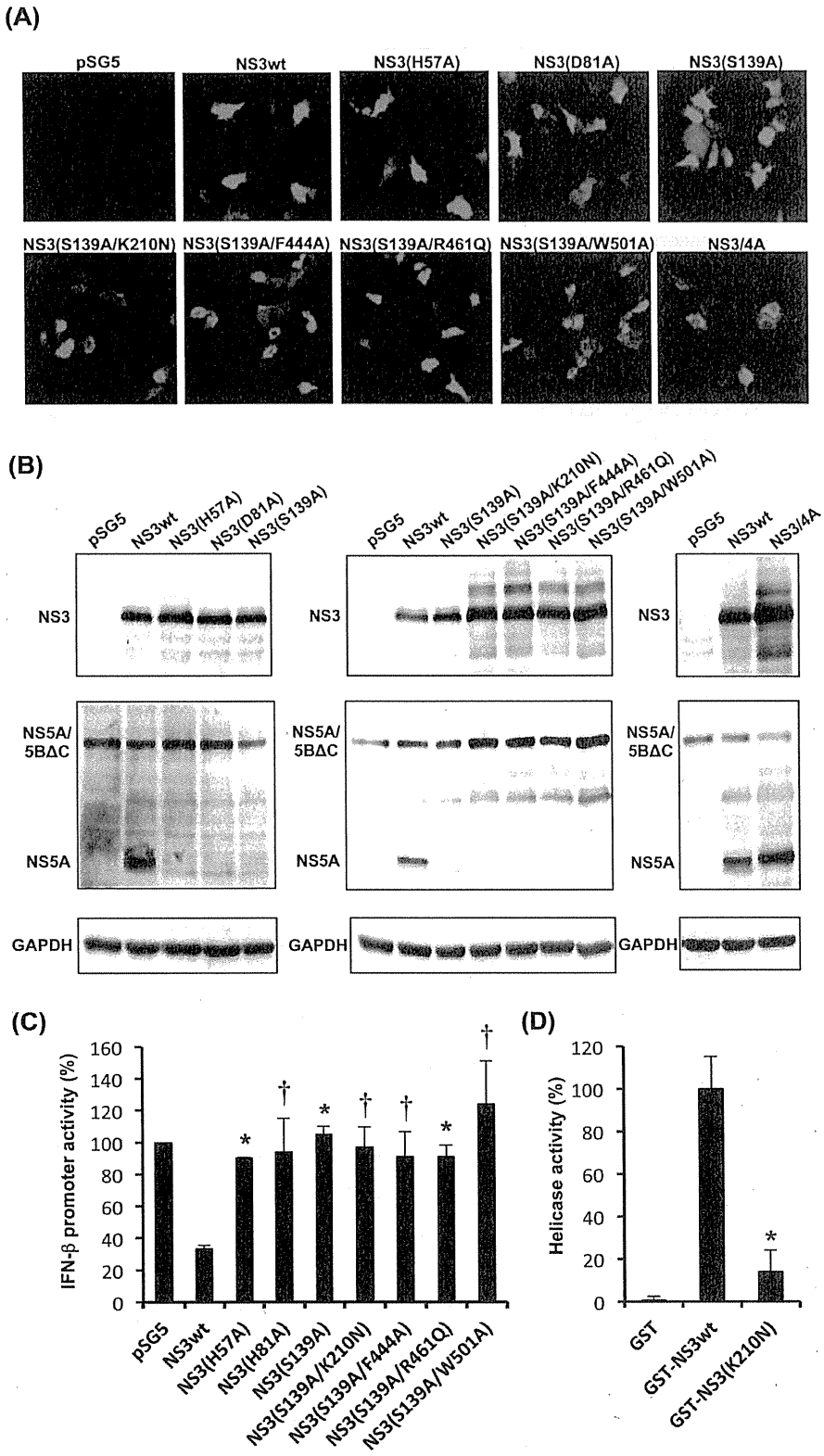

Figure 2. Analysis of NS3 expression, serine protease activity, effects on IFN-β promoter activity and RNA helicase activity. (A) Immunofluorescence analysis of NS3wt, various NS3 mutants and NS3/4A in Huh-7.5 cells transfected with the DNA vaccine candidates using anti-

NS3 monoclonal antibody. (B) Serine protease analysis of NS3wt, various NS3 mutants and NS3/4A. Huh-7.5 cells were transiently transfected with each of the NS3 expression plasmids together with pNS5A/5BΔC (as a substrate). Cell lysates were subjected to immunoblot analysis using anti-NS3 and anti-NS5A monoclonal antibodies to detect NS3 (top panel) and NS5A/5BΔC and NS5A (middle panel), respectively. The amounts of GAPDH (bottom panel) were measured as an internal control to verify equal amounts of sample loading. (C) Effects of NS3wt or NS3 mutants on RIG-I-mediated IFN-β promoter activity. Huh-7 cells were transfected with a plasmid expressing NS3wt or each NS3 mutant together with pSG5-NS4A, pEF1A/N-RIG-I-FLAG, pIFN-β-luc and pRL-TK. Firefly luciferase activity was measured 48 h post transfection and normalized to Renilla luciferase activity. Data represent mean ± SEM of the data from three independent experiments. *, $p<0.01$; †, $p<0.05$, compared with NS3wt. (D) RNA helicase analysis of NS3wt and its mutant. NS3 helicase assay was performed using GST-NS3wt, GST-NS3(K210N) and GST as a negative control, as described in the Materials and methods section. The mean activity obtained with the GST control was subtracted from those obtained with test samples. The mean activity of GST-NS3wt was arbitrarily expressed as 100%. *, $p<0.05$, compared with NS3wt.
doi:10.1371/journal.pone.0098877.g002

were carried out for 60 min at 37°C. To stop the reactions, the wells were washed with 150 mM NaCl and dried at room temperature for 15 min. The wells were then washed with a detection washing buffer (100 mM maleic acid, 150 mM NaCl and 0.3% Tween 20, pH 7.5), incubated with a 10% BSA-containing blocking solution (100 mM maleic acid and 150 mM NaCl, pH 7.5) for 30 min followed by incubation with 20 μl of alkaline phosphatase-labeled anti-digoxygenin antibody solution (Roche Applied Science, Germany; 1:10,000 dilution in the blocking solution) for 30 min. After being washed with a detection buffer (100 mM Tris-HCl, pH 9.5, and 100 mM NaCl), 20 μl of a working solution containing CSPD chemiluminescence substrate (Roche) was added to each well and the plates were incubated for 5 min at 17°C. The wells were then drained and dried, and the luminescence in each well was counted in a luminescence multi-well plate reader. Helicase activities were determined by the reduction of the luminescence, which reflects the release of the digoxygenin-labeled oligonucleotides from the otherwise DNA duplex substrate.

Luciferase Reporter Assay

Huh-7 cells cultured in a 24-well tissue culture plate were transiently transfected with pSG5-NS3wt or each NS3 mutant (0.25 μg), together with pSG5-NS4A (0.25 μg), pIFN-β-Luc (0.2 μg), pEF1A/N-RIG-I-FLAG (0.05 μg) and pRL-TK (0.01 μg). After 48 h, cells were harvested and a luciferase assay was performed by using Dual-Luciferase Reporter Assay system (Promega). Firefly and Renilla luciferase activities were measured by using a GloMax 96 Microplate Luminometer (Promega).

Mice and Immunizations

BALB/c mice (H-2^d) were purchased from CLEA Japan, Inc. Mice were maintained in specific pathogen-free conditions according to institutional guidelines. All of the animal experiments were carried out according to the protocol approved by the Ethics Committee for Animal Experiments at Kobe University (Permit Number: P121002). All surgery was performed under isoflurane anesthesia, and efforts were made to minimize suffering. Eight-week-old female BALB/c mice were immunized with 200 μg of a plasmid, 100 μg each into both quadriceps, by intramuscular

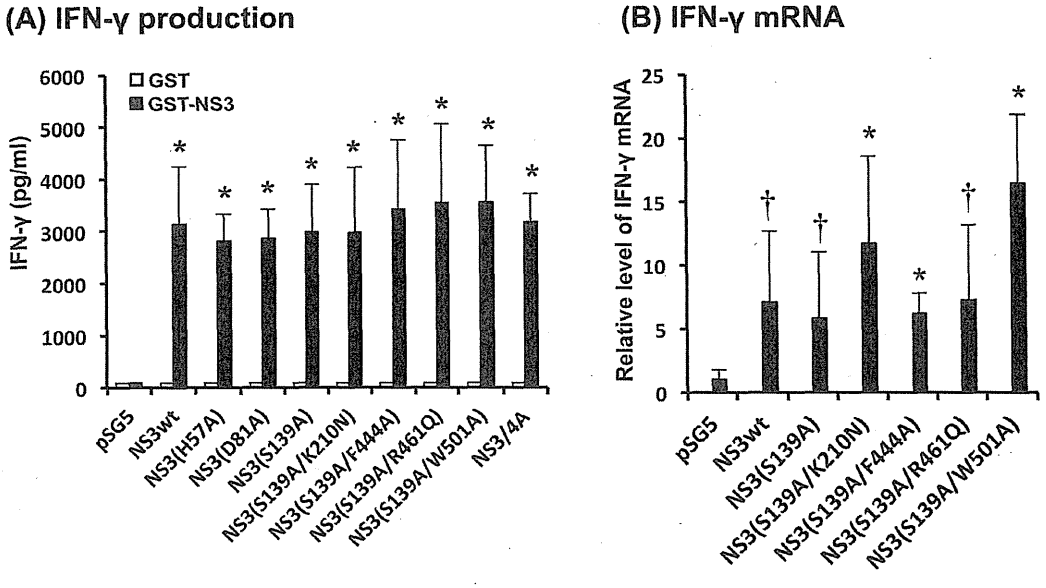

Figure 3. IFN-γ production induced by NS3 DNA vaccination. (A) IFN-γ production by splenocytes obtained from immunized mice. BALB/c mice (2 mice/group) were immunized with each of the DNA vaccines expressing NS3wt, various NS3 mutants or NS3/4A. Splenocytes obtained from the immunized mice were cultured in the presence of GST-NS3 (5 μg/ml) for 72 h. The amounts of IFN-γ in culture supernatants were measured with ELISA. Data represent mean ± SEM of the data from three independent experiments. *, $p<0.01$ compared with the mock-immunized control. (B) IFN-γ mRNA expression. Splenocytes obtained from immunized mice were cultured in the presence of GST-NS3 (5 μg/ml) for 24 h. The amounts of IFN-γ mRNA were determined by real-time quantitative RT-PCR analysis and normalized to GAPDH mRNA expression levels. Data represent mean ± SEM of the data from three independent experiments. The value for splenocytes from the mock-immunized control was arbitrarily expressed as 1.0. *, $p<0.01$; †, $p<0.05$, compared with the control.
doi:10.1371/journal.pone.0098877.g003

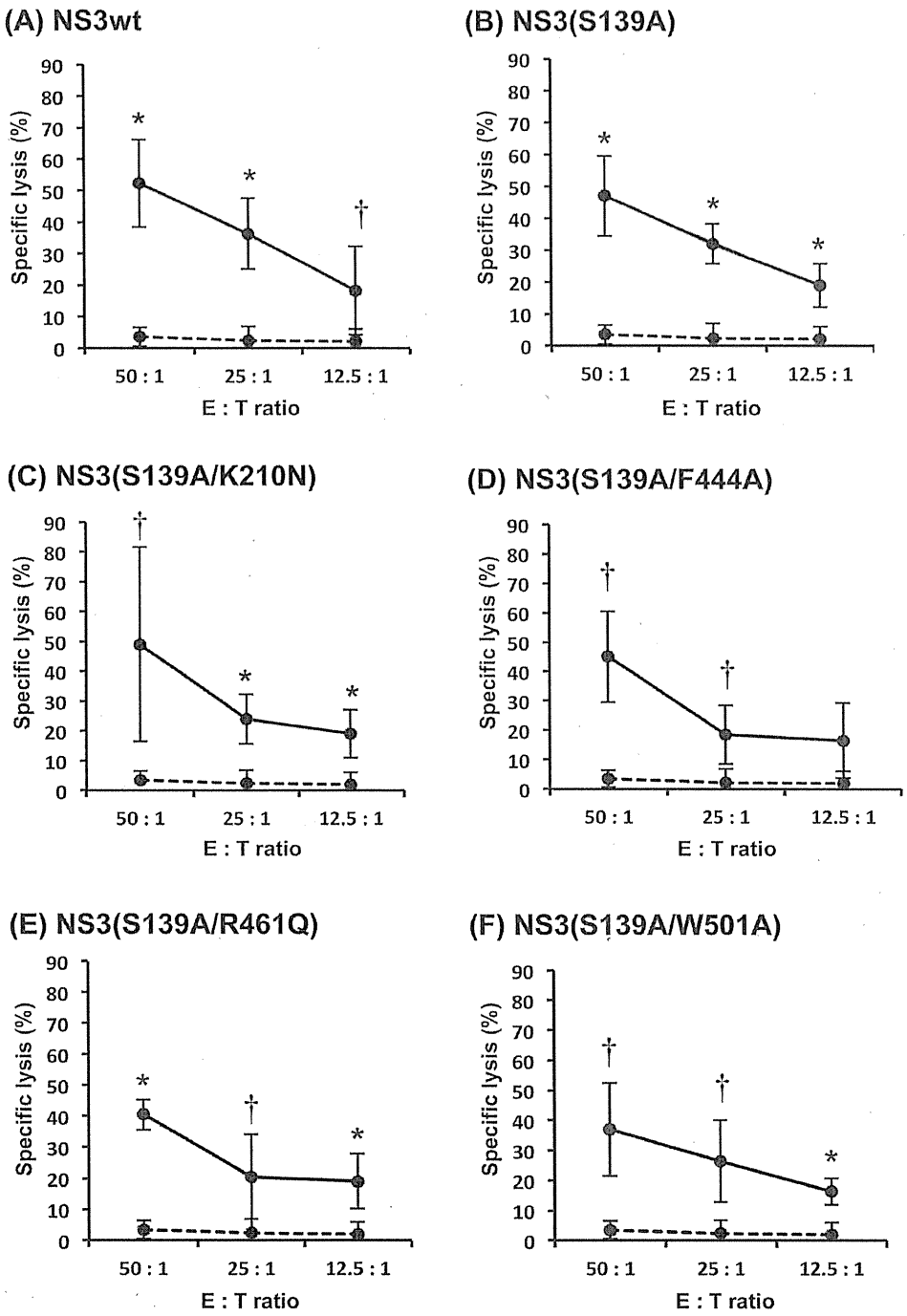

Figure 4. NS3-specific CTL activity induced by DNA vaccination. BALB/c mice (2 mice/group) were immunized with each of the DNA vaccines expressing NS3wt, various NS3 mutants or NS3/4A. Splenocytes obtained from the immunized mice were stimulated in vitro for 5 days with P815-NS3 cells and GST-NS3wt (5 μg/ml). Effectors and targets (P815-NS3) were cocultured for 4 h with the ratios of 50:1, 25:1, and 12.5:1. Released LDH was measured and the percentage of specific killing was calculated. Specific CTL activity of splenocytes obtained from NS3-immunized mice and the mock-immunized control are shown with solid and dashed lines, respectively. Data represent mean ± SEM of the data from three independent experiments. *, $p<0.01$; †, $p<0.05$, compared with the mock-immunized control.
doi:10.1371/journal.pone.0098877.g004

injection using a needle-free injector (Twin-Jector EZ II, JCR Pharmaceuticals Co., Ltd., Japan). We adopted the injection dosage according to previous studies [41,42]. The needle-free jet injection has been reported to enhance the immunological

responses induced by DNA vaccines [43]. Mice were boosted with the same plasmid (100 μg) at 4 and 6 weeks after the first injection. Control mice were injected with the empty pSG5 vector.

Splenocytes Culture

Eight weeks after the first immunization, spleens were resected and crushed with the use of a 22G needle. Splenocytes were strained with a cell strainer (40 μM, BD Falcon, USA) and treated for 5 min with 0.75% ammonium chloride buffer (pH 7.65) to lyse red blood cells. The splenocytes were suspended in RPMI1640 medium supplemented with 2 mM L-glutamine, 10% heat inactivated FCS, 50 U/ml penicillin, 50 U/ml streptomycin and 55 mM 2-mercaptoethanol.

IFN-γ Secretion Assay

Splenocytes seeded in 96-well (flat-bottom) plates at a concentration of 4×10^5 cells per well in 200 μl complete medium were stimulated with GST-NS3, or GST as a control, at a concentration of 5 μg/ml for 72 h. The amounts of IFN-γ in the culture supernatants were measured using an ELISA kit (Quantikine Mouse IFN-γ, R&D System, Minneapolis, MN, USA) according to the manufacturer's instructions.

Real-time Quantitative RT-PCR

Total RNA was extracted from GST-NS3-stimulated mouse splenocytes using a ReliaPrep RNA cell miniprep system (Promega) according to the manufacturer's instructions. One μg of total RNA was reverse transcribed using a GoScript Reverse Transcription system (Promega) with random primers and was subjected to quantitative real-time PCR analysis using SYBR Premix Ex Taq (TaKaRa Bio Inc., Kyoto, Japan) in a MicroAmp 96-well reaction plate and an Applied Biosystems 7500 fast Real-time PCR system (Applied Biosystems, Foster City, CA, USA). The primers used to amplify IFN-γ mRNA were 5-CCTGCGGCCTAGCTCTGA-3′ (sense) and 5′-CAGCCA-GAAACAGCCATGAG-3′ (antisense). As an internal control, murine glyceraldehyde-3-phosphate dehydrogenase (GAPDH) mRNA levels were measured using primers 5′-CATCGCCTTCCGTGTTCCTA-3′ (sense) and 5′-GCGGCACGTCAGATCCA-3′ (antisense).

CTL Assay

Splenocytes obtained from NS3-immunized mice were cultured for 5 days with P815-NS3 cells and 5 μg/ml of GST-NS3 to generate effector cells. The effector splenocytes and target P815-NS3 cells (1×10^4 cells) were cocultured in 96-well plates (round-bottom) for 4 h at 37°C in 5% CO_2 with ratios of 50:1, 25:1, and 12.5:1. Specific CTL activity was measured using a Lactate Dehydrogenase (LDH) Cytotoxicity Assay Kit (CytoTox 96 Non-Radioactive Cytotoxicity Assay; Promega). Released LDH was measured according to the manufacturer's protocol. The percentage of specific killing was calculated by the following formula: % specific killing = (experimental release − effector spontaneous release − target spontaneous release)/(target maximum release − target spontaneous release)×100.

Statistical Analysis

Student's t-test was used to compare the data between two different groups. For multiple comparisons, a one-way analysis of variance (ANOVA) was used. A p-value of <0.05 was considered to be statistically significant.

Results

Characterization of Wild Type NS3 (NS3wt) and NS3 Mutants Expressed by DNA Vaccines

We constructed plasmids expressing NS3 mutants lacking the serine protease and the NTPase/RNA helicase activities to avoid potential risks posed by those enzymes (Fig. 1). The NS3 mutants were expressed efficiently in Huh-7.5 cells, as demonstrated by immunofluorescence (Fig. 2A) and immunoblotting assays (Fig. 2B, top panel). Importantly, all the NS3 mutants, either protease-deficient single-mutants or protease/helicase-deficient double-mutants, lacked the serine protease activity, as shown by the absence of the cleaved-off product of NS5A (Fig. 2B, middle panel). Equal loading of the samples was verified by GAPDH staining (Fig. 2B, bottom panel). The serine protease activity of NS3 is also known to cleave the RIG-I-associated adaptor protein MAVS (also known as Cardif, IPS-1 and VISA) and, therefore, blockade the RIG-I-mediated induction of IFN-β gene expression [44,45]. We confirmed that all the NS3 mutants lost their abilities to blockade the RIG-I-mediated IFN-β gene expression (Fig. 2C).

As for the NTPase/RNA helicase activities of NS3, it has been well documented that introduction of either one of the K210N, F444A, R461Q and W501A mutations severely affects the NS3 helicase activity [34,35,36]. Indeed, we confirmed that NS3 helicase activity was markedly impaired by the introduction of the K210N mutation (Fig. 2D).

Induction of IFN-γ Production by NS3-specific T cells after Immunization with NS3 DNA Vaccines

In order to evaluate the possible efficacy of the NS3 plasmids as DNA vaccines, BALB/c mice were injected intramuscularly with each of the plasmids, followed by booster injections at 4 and 6 weeks after the first injection. Two weeks after the last immunization, splenocytes were obtained from the mice, stimulated with GST-NS3 *in vitro* and the levels of IFN-γ production in the culture supernatants were measured. The results obtained revealed that protease-deficient single-mutants, i.e., NS3(H57A), NS3(D81A) and NS3(S139A), induced high levels of IFN-γ production, which were comparable to that induced by NS3wt and NS3/4A (Fig. 3A). Moreover, protease/helicase-deficient double-mutants with the backbone of NS3(S139A), i.e., NS3(S139A/K210N), NS3(S139A/F444A), NS3(S139A/R461Q) and NS3(S139A/W501A), induced IFN-γ production to the same extent as observed with the single-mutants. Consistently, real-time quantitative RT-PCR analysis revealed that the levels of IFN-γ mRNA expression were significantly higher in splenocytes obtained from NS3-immunized mice than those from mock-immunized control (Fig. 3B).

Induction of NS3-specific CTL Activities by Immunization with NS3 DNA Vaccines

We measured CTL activities induced by the NS3 DNA vaccines. Splenocytes obtained from the vaccinated mice two weeks after the last immunization were stimulated with GST-NS3 and P815-NS3 cells for 5 days and the effector splenocytes were mixed with the target P815-NS3 cells to determine the levels of CTL activities. Protease/helicase-deficient double-mutants, NS3(S139A/K210N), NS3(S139A/F444A), NS3(S139A/R461Q) and NS3(S139A/W501A), induced strong CTL activities against the target P815-NS3 cells to the level equivalent to that induced by NS3wt and a protease-deficient single-mutant NS3(S139A) (Fig. 4).

Discussion

Effective therapeutic vaccines against virus infection must induce sufficient levels of cell-mediated immune responses against the target viral epitope(s) and also must avoid concomitant risk factors, including potential carcinogenic properties. The HCV NS3 is considered to be an important target for development of HCV therapeutic vaccines because NS3-specific $CD4^+$ and $CD8^+$ T cell responses correlate well with resolution of the infection [46,47,48] and have been described as an indicator for viral clearance both in humans and chimpanzees [48,49,50]. On the other hand, NS3 possesses serine protease and NTPase/RNA helicase activities, which are necessary for the viral polyprotein processing and viral RNA replication, respectively [1,2]. In addition to the essential role in the virus life cycle, the NS3 serine protease interferes with normal cellular functions, such as blockade of IFN-β production [3,18,19,20] and deregulation of EGF signaling [22]. Also, the NTPase/RNA helicase of NS3 may interferes with cellular RNA helicases, which are involved in RNA folding/remodeling [51], enhancement of polymerase processivity [52], and/or genome encapsidation [53]. Importantly, perturbations of cellular RNA helicases are implicated in cancer development [23]. In the present study, therefore, we aimed to develop DNA vaccines that express NS3 mutants lacking both serine protease and NTPase/RNA helicase activities (Fig. 1) in order to avoid concomitant potential risks caused by the viral enzymes.

We first introduced single-point mutations into each of the catalytic triad of the NS3 serine protease (H57A, D81A and S139A) and found that all of the NS3 mutants efficiently induced IFN-γ production by splenocytes obtained from the vaccinated mice (Fig. 3A). Since His at position 57 is located within a well-characterized $CD4^+/CD8^+$ epitope [14,54], we decided not to choose pNS3(H57A) as a vaccine candidate. We then introduced a point mutation (K210N, F444A, R461Q and W501A) [34,35,36] to pNS3(S139A) to impair NTPase/RNA helicase activities. All the resultant DNA vaccine candidates, pNS3(S139A/K210N), pNS3(S139A/F444A), pNS3(S139A/R461Q) and pNS3(S139A/W501A), which express double-mutants lacking both serine protease and NTPase/RNA helicase activities, efficiently induced IFN-γ production by splenocytes of the vaccinated mice. We also observed that the protease-deficient single-mutant pNS3(S139A) and all of the four protease/helicase-deficient double-mutants induced NS3-specific CTL activities to the same extent compared to the non-mutated pNS3wt (Fig. 4). All but H57A mutation of NS3 examined in this study are located outside the human CD4 and CD8 epitopes reported so far, with the H57A mutation being located at the C-terminal edge of an epitope [7,8,9,11]. Therefore, these findings suggest that a single mutation in the protease and NTPase/RNA helicase domains would not interfere with immunogenicity of NS3 as a whole in mice and human.

In general, DNA vaccines mediate antigen expression only transiently in the vaccinees and, therefore, the possible side effects caused by the NS3 enzymatic activities through DNA vaccination would be rather marginal. However, when NS3 is expressed by means of a long-lasting live vaccine, such as a recombinant attenuated varicella zoster virus vaccine, it might potentially exert certain harmful effects after a long period of time. Currently, we aim to generate a recombinant attenuated varicella zoster virus expressing HCV NS3. For this purpose, an NS3 mutant lacking both protease and helicase activities and yet maintaining a full range of antigenic epitopes would be more appropriate than NS3wt.

In summary, we propose that plasmids expressing NS3 protease/helicase-deficient double-mutants, pNS3(S139A/K210N), pNS3(S139A/F444A), pNS3(S139A/R461Q) and pNS3(S139A/W501A), would be good candidates for safe and efficient therapeutic DNA vaccines against HCV infection.

Acknowledgments

The authors are grateful to Dr. T. Fujita, Kyoto University, for providing pIFNβ-Luc.

Author Contributions

Conceived and designed the experiments: SLR DPJ CA PS LD HH. Performed the experiments: SLR DPJ IS LD. Analyzed the data: SLR DPJ. Contributed reagents/materials/analysis tools: HH. Wrote the paper: SLR DPJ HH.

References

1. Lindenbach BD, Rice CM (2005) Unravelling hepatitis C virus replication from genome to function. Nature 436: 933–938.
2. Scheel TK, Rice CM (2013) Understanding the hepatitis C virus life cycle paves the way for highly effective therapies. Nat Med 19: 837–849.
3. Morikawa K, Lange CM, Gouttenoire J, Meylan E, Brass V, et al. (2011) Nonstructural protein 3–4A: the Swiss army knife of hepatitis C virus. J Viral Hepat 18: 305–315.
4. Micallef JM, Kaldor JM, Dore GJ (2006) Spontaneous viral clearance following acute hepatitis C infection: a systematic review of longitudinal studies. J Viral Hepat 13: 34–41.
5. Mohd Hanafiah K, Groeger J, Flaxman AD, Wiersma ST (2013) Global epidemiology of hepatitis C virus infection: new estimates of age-specific antibody to HCV seroprevalence. Hepatology 57: 1333–1342.
6. Zeuzem S, Andreone P, Pol S, Lawitz E, Diago M, et al. (2011) Telaprevir for retreatment of HCV infection. N Engl J Med 364: 2417–2428.
7. Castelli FA, Leleu M, Pouvelle-Moratille S, Farci S, Zarour HM, et al. (2007) Differential capacity of T cell priming in naive donors of promiscuous CD4+ T cell epitopes of HCV NS3 and Core proteins. Eur J Immunol 37: 1513–1523.
8. Mashiba T, Udaka K, Hirachi Y, Hiasa Y, Miyakawa T, et al. (2007) Identification of CTL epitopes in hepatitis C virus by a genome-wide computational scanning and a rational design of peptide vaccine. Immunogenetics 59: 197–209.
9. Day CL, Lauer GM, Robbins GK, McGovern B, Wurcel AG, et al. (2002) Broad specificity of virus-specific CD4+ T-helper-cell responses in resolved hepatitis C virus infection. J Virol 76: 12584–12595.
10. Bowen DG, Walker CM (2005) Adaptive immune responses in acute and chronic hepatitis C virus infection. Nature 436: 946–952.
11. Takaki A, Wiese M, Maertens G, Depla E, Seifert U, et al. (2000) Cellular immune responses persist and humoral responses decrease two decades after recovery from a single-source outbreak of hepatitis C. Nat Med 6: 578–582.
12. Penna A, Missale G, Lamonaca V, Pilli M, Mori C, et al. (2002) Intrahepatic and circulating HLA class II-restricted, hepatitis C virus-specific T cells: functional characterization in patients with chronic hepatitis C. Hepatology 35: 1225–1236.
13. MacDonald AJ, Duffy M, Brady MT, McKiernan S, Hall W, et al. (2002) CD4 T helper type 1 and regulatory T cells induced against the same epitopes on the core protein in hepatitis C virus-infected persons. J Infect Dis 185: 720–727.
14. Wedemeyer H, He XS, Nascimbeni M, Davis AR, Greenberg HB, et al. (2002) Impaired effector function of hepatitis C virus-specific CD8+ T cells in chronic hepatitis C virus infection. J Immunol 169: 3447–3458.
15. Moriya K, Fujie H, Shintani Y, Yotsuyanagi H, Tsutsumi T, et al. (1998) The core protein of hepatitis C virus induces hepatocellular carcinoma in transgenic mice. Nat Med 4: 1065–1067.
16. Levrero M (2006) Viral hepatitis and liver cancer: the case of hepatitis C. Oncogene 25: 3834–3847.
17. Banerjee A, Ray RB, Ray R (2010) Oncogenic potential of hepatitis C virus proteins. Viruses 2: 2108–2133.
18. Gale M Jr, Foy EM (2005) Evasion of intracellular host defence by hepatitis C virus. Nature 436: 939–945.
19. Lindenbach BD, Evans MJ, Syder AJ, Wolk B, Tellinghuisen TL, et al. (2005) Complete replication of hepatitis C virus in cell culture. Science 309: 623–626.
20. Foy E, Li K, Sumpter R Jr, Loo YM, Johnson CL, et al. (2005) Control of antiviral defenses through hepatitis C virus disruption of retinoic acid-inducible gene-I signaling. Proc Natl Acad Sci U S A 102: 2986–2991.

21. Kaukinen P, Sillanpaa M, Kotenko S, Lin R, Hiscott J, et al. (2006) Hepatitis C virus NS2 and NS3/4A proteins are potent inhibitors of host cell cytokine/chemokine gene expression. Virol J 3: 66.
22. Brenndorfer ED, Karthe J, Frelin L, Cebula P, Erhardt A, et al. (2009) Nonstructural 3/4A protease of hepatitis C virus activates epithelial growth factor-induced signal transduction by cleavage of the T-cell protein tyrosine phosphatase. Hepatology 49: 1810–1820.
23. Robert F, Pelletier J (2013) Perturbations of RNA helicases in cancer. Wiley Interdiscip Rev RNA 4: 333–349.
24. Botlagunta M, Vesuna F, Mironchik Y, Raman A, Lisok A, et al. (2008) Oncogenic role of DDX3 in breast cancer biogenesis. Oncogene 27: 3912–3922.
25. Abdelhaleem M (2004) Do human RNA helicases have a role in cancer? Biochim Biophys Acta 1704: 37–46.
26. Hidajat R, Nagano-Fujii M, Deng L, Tanaka M, Takigawa Y, et al. (2005) Hepatitis C virus NS3 protein interacts with ELKS-{delta} and ELKS-{alpha}, members of a novel protein family involved in intracellular transport and secretory pathways. J Gen Virol 86: 2197–2208.
27. Deng L, Nagano-Fujii M, Tanaka M, Nomura-Takigawa Y, Ikeda M, et al. (2006) NS3 protein of Hepatitis C virus associates with the tumour suppressor p53 and inhibits its function in an NS3 sequence-dependent manner. J Gen Virol 87: 1703–1713.
28. Yoneyama M, Kikuchi M, Natsukawa T, Shinobu N, Imaizumi T, et al. (2004) The RNA helicase RIG-I has an essential function in double-stranded RNA-induced innate antiviral responses. Nat Immunol 5: 730–737.
29. Love RA, Parge HE, Wickersham JA, Hostomsky Z, Habuka N, et al. (1996) The crystal structure of hepatitis C virus NS3 proteinase reveals a trypsin-like fold and a structural zinc binding site. Cell 87: 331–342.
30. Lin C, Pragai BM, Grakoui A, Xu J, Rice CM (1994) Hepatitis C virus NS3 serine proteinase: trans-cleavage requirements and processing kinetics. J Virol 68: 8147–8157.
31. Grakoui A, McCourt DW, Wychowski C, Feinstone SM, Rice CM (1993) Characterization of the hepatitis C virus-encoded serine proteinase: determination of proteinase-dependent polyprotein cleavage sites. J Virol 67: 2832–2843.
32. Tomei L, Failla C, Santolini E, De Francesco R, La Monica N (1993) NS3 is a serine protease required for processing of hepatitis C virus polyprotein. J Virol 67: 4017–4026.
33. Martinez MA, Clotet B (2003) Genetic screen for monitoring hepatitis C virus NS3 serine protease activity. Antimicrob Agents Chemother 47: 1760–1765.
34. Frick DN (2007) The hepatitis C virus NS3 protein: a model RNA helicase and potential drug target. Curr Issues Mol Biol 9: 1–20.
35. Kuang WF, Lin YC, Jean F, Huang YW, Tai CL, et al. (2004) Hepatitis C virus NS3 RNA helicase activity is modulated by the two domains of NS3 and NS4A. Biochem Biophys Res Commun 317: 211–217.
36. Tai CL, Pan WC, Liaw SH, Yang UC, Hwang LH, et al. (2001) Structure-based mutational analysis of the hepatitis C virus NS3 helicase. J Virol 75: 8289–8297.
37. Blight KJ, McKeating JA, Rice CM (2002) Highly permissive cell lines for subgenomic and genomic hepatitis C virus RNA replication. J Virol 76: 13001–13014.
38. Deng L, Shoji I, Ogawa W, Kaneda S, Soga T, et al. (2011) Hepatitis C virus infection promotes hepatic gluconeogenesis through an NS5A-mediated, FoxO1-dependent pathway. J Virol 85: 8556–8568.
39. Hicham Alaoui-Ismaili M, Gervais C, Brunette S, Gouin G, Hamel M, et al. (2000) A novel high throughput screening assay for HCV NS3 helicase activity. Antiviral Res 46: 181–193.
40. Vlachakis D, Brancale A, Berry C, Kossida S (2011) A rapid assay for the biological evaluation of helicase activity. Protocol Exchange doi:10.1038/protex.2011.275. http://www.nature.com/protocolexchange/protocols/2282#/.
41. Hegde R, Liu Z, Mackay G, Smith M, Chebloune Y, et al. (2005) Antigen expression kinetics and immune responses of mice immunized with noninfectious simian-human immunodeficiency virus DNA. J Virol 79: 14688–14697.
42. Zhou F, Wang G, Buchy P, Cai Z, Chen H, et al. (2012) A triclade DNA vaccine designed on the basis of a comprehensive serologic study elicits neutralizing antibody responses against all clades and subclades of highly pathogenic avian influenza H5N1 viruses. J Virol 86: 6970–6978.
43. Raviprakash K, Porter KR (2006) Needle-free injection of DNA vaccines: a brief overview and methodology. Methods Mol Med 127: 83–89.
44. Sumpter R Jr, Loo YM, Foy E, Li K, Yoneyama M, et al. (2005) Regulating intracellular antiviral defense and permissiveness to hepatitis C virus RNA replication through a cellular RNA helicase, RIG-I. J Virol 79: 2689–2699.
45. Moradpour D, Penin F, Rice CM (2007) Replication of hepatitis C virus. Nat Rev Microbiol 5: 453–463.
46. Diepolder HM, Gerlach JT, Zachoval R, Hoffmann RM, Jung MC, et al. (1997) Immunodominant CD4+ T-cell epitope within nonstructural protein 3 in acute hepatitis C virus infection. J Virol 71: 6011–6019.
47. Diepolder HM, Zachoval R, Hoffmann RM, Wierenga EA, Santantonio T, et al. (1995) Possible mechanism involving T-lymphocyte response to non-structural protein 3 in viral clearance in acute hepatitis C virus infection. Lancet 346: 1006–1007.
48. Missale G, Bertoni R, Lamonaca V, Valli A, Massari M, et al. (1996) Different clinical behaviors of acute hepatitis C virus infection are associated with different vigor of the anti-viral cell-mediated immune response. J Clin Invest 98: 706–714.
49. Thimme R, Oldach D, Chang KM, Steiger C, Ray SC, et al. (2001) Determinants of viral clearance and persistence during acute hepatitis C virus infection. J Exp Med 194: 1395–1406.
50. Nascimbeni M, Mizukoshi E, Bosmann M, Major ME, Mihalik K, et al. (2003) Kinetics of CD4+ and CD8+ memory T-cell responses during hepatitis C virus rechallenge of previously recovered chimpanzees. J Virol 77: 4781–4793.
51. Rajkowitsch L, Chen D, Stampfl S, Semrad K, Waldsich C, et al. (2007) RNA chaperones, RNA annealers and RNA helicases. RNA Biol 4: 118–130.
52. Jarvis TC, Kirkegaard K (1991) The polymerase in its labyrinth: mechanisms and implications of RNA recombination. Trends Genet 7: 186–191.
53. Sun S, Rao VB, Rossmann MG (2010) Genome packaging in viruses. Curr Opin Struct Biol 20: 114–120.
54. Wertheimer AM, Miner C, Lewinsohn DM, Sasaki AW, Kaufman E, et al. (2003) Novel CD4+ and CD8+ T-cell determinants within the NS3 protein in subjects with spontaneously resolved HCV infection. Hepatology 37: 577–589.

Microbiology and Immunology

Microbiol Immunol 2014; 58: 188–194
doi: 10.1111/1348-0421.12133

ORIGINAL ARTICLE

Antiviral activity of extracts from *Morinda citrifolia* leaves and chlorophyll catabolites, pheophorbide a and pyropheophorbide a, against hepatitis C virus

Suratno Lulut Ratnoglik[1], Chie Aoki[1,2], Pratiwi Sudarmono[4], Mari Komoto[1], Lin Deng[1], Ikuo Shoji[1], Hiroyuki Fuchino, Nobuo Kawahara and Hak Hotta[1]

[1]Division of Microbiology, Kobe University Graduate School of Medicine, 7-5-1 Kusunoki-cho, Chuo-ku, Kobe 650 0017, Japan, [2]JST/JICA within the Science and Technology Research Partnership for Sustainable Development Laboratory, Tokyo, Japan, [3]Faculty of Medicine, University of Indonesia Jl., Salemba 4, Jakarta 10430, Indonesia and [4]Research Center for Medicinal Plant Resources, National Institute of Biomedical Innovation, 1-2 Hachimandai, Tsukuba Ibaraki 305 0843, Japan

ABSTRACT

The development of complementary and/or alternative drugs for treatment of hepatitis C virus (HCV) infection is still needed. Antiviral compounds in medicinal plants are potentially good targets to study. *Morinda citrifolia* is a common plant distributed widely in Indo-Pacific region; its fruits and leaves are food sources and are also used as a treatment in traditional medicine. In this study, using a HCV cell culture system, it was demonstrated that a methanol extract, its *n*-hexane, and ethyl acetate fractions from *M. citrifolia* leaves possess anti-HCV activities with 50%-inhibitory concentrations (IC_{50}) of 20.6, 6.1, and 6.6 μg/mL, respectively. Bioactivity-guided purification and structural analysis led to isolation and identification of pheophorbide a, the major catabolite of chlorophyll a, as an anti-HCV compound present in the extracts (IC_{50} = 0.3 μg/mL). It was also found that pyropheophorbide a possesses anti-HCV activity (IC_{50} = 0.2 μg/mL). The 50%-cytotoxic concentrations (CC_{50}) of pheophorbide a and pyropheophorbide a were 10.0 and 7.2 μg/mL, respectively, their selectivity indexes being 33 and 36, respectively. On the other hand, chlorophyll a, sodium copper chlorophyllin, and pheophytin a barely, or only marginally, exhibited anti-HCV activities. Time-of-addition analysis revealed that pheophorbide a and pyropheophorbide a act at both entry and the post-entry steps. The present results suggest that pheophorbide a and its related compounds would be good candidates for seed compounds for developing antivirals against HCV.

Key words antiviral, hepatitis C virus, pheophorbide a, pyropheophorbide a.

Hepatitis C virus (HCV) belongs to the *Hepacivirus* genus within the *Flaviviridae* family. The viral genome, a single-stranded, positive-sense RNA of 9.6 kb, encodes a polyprotein precursor consisting of about 3000 amino acid residues (1). The polyprotein is cleaved by the host and viral proteases to generate 10 mature proteins, namely core, envelope (E) 1, E2, a putative ion channel p7, and nonstructural proteins NS2, NS3, NS4A, NS4B, NS5A and NS5B. Core, E1, and E2 are the structural proteins and form the infectious virus particle together with the viral genome. The nonstructural proteins play essential roles in viral RNA replication. Based on a considerable degree of sequence heterogeneity of its genome, HCV is currently classified into seven genotypes (1–7) and more than 70 subtypes (1a, 1b, 2a, 2b, etc.) (2).

Correspondence
Hak Hotta, Division of Microbiology, Kobe University Graduate School of Medicine, 7-5-1 Kusunoki-cho, Chuo-ku, Kobe 650 0017, Japan. Tel:+81 78 382 5500; fax: +81 78 382 5519; e-mail: hotta@kobe-u.ac.jp

Received 8 January 2014; revised 11 January 2014; accepted 16 January 2014.

List of Abbreviations: CC_{50}, 50%-cytotoxic concentrations; dpi, days post-infection; FR., fraction; GAPDH, glyceraldehyde-3-phosphate dehydrogenase; HCV, hepatitis C virus; IC_{50}, 50%-inhibitory concentration; ID, internal diameter; NMR, nuclear magnetic resonance; ODS, octadecyl silane; SI, selectivity index; TLC, thin layer chromatography.

Hepatitis C virus is a major cause of chronic liver diseases, such as hepatitis, cirrhosis, and hepatocellular carcinoma, with substantial morbidity and mortality (3, 4). The prevalence of HCV is about 2%, representing 120 million people worldwide. Current standard treatment using pegylated interferon and ribavirin is effective in only half the patients infected with HCV genotype 1, which is the most resistant of all HCV genotypes to interferon-based therapy. Therefore, development of complementary and/or alternative drugs for treatment of HCV infection is still needed from both clinical and economic points of view. In this regard, antiviral substances obtained from medicinal plants are potentially good targets to study (5–7), as has also been reported for other viruses (8).

Morinda citrifolia belongs to the Rubiaceae family and is thought to have originated in Indonesia. This common plant is distributed widely in the Indo-Pacific region. The fruits and leaves of *M. citrifolia* are food sources for local people and are also used as a treatment for infections and inflammatory diseases (9) in traditional medicine. Nowadays, the juice from the ripe fruits, traditionally known as "noni," is sold as a health food even in industrialized countries. It has been reported that methanol or ethanol extracts of *M. citrifolia* fruits and/or leaves have antibacterial activities against some bacteria, such as *Staphylococcus aureus* (10) and *Mycobacterium tuberculosis* (11). Using an HCV subgenomic replicon, anti-HCV activity has also been reported for both methanol and ethanol extracts of *M. citrifolia* fruits (12). In this study, we used an HCV infection system in cultured cells to explore the anti-HCV activities of methanol extracts of the fruits (ripe and frozen), leaves, roots, and branches of *M. citrifolia*. We report here that a methanol extract of *M. citrifolia* leaves and its subfractions, as well as an isolated compound, pheophorbide a, and its catabolite, pyropheophorbide a, possess antiviral activities against HCV.

MATERIALS AND METHODS

Cells and viruses

Huh7.5 cells and the plasmid pFL-J6/JFH1 to produce the J6/JFH1 strain of HCV genotype 2a (13) were kindly provided by Dr. C.M. Rice (Rockefeller University, New York, NY, USA). The J6/JFH1-P47 strain of HCV was prepared as described previously (14). Huh7.5 cells were cultured in Dulbecco's modified Eagle's medium (Wako, Osaka, Japan) supplemented with FBS (Biowest, Nuaillé, France), non-essential amino acids (Invitrogen, Carlsbad, CA, USA), penicillin (100 IU/mL), and streptomycin (100 μg/mL) (Invitrogen) at 37 °C in a 5% CO_2 incubator.

Extraction of various parts of *M. citrifolia* and further fractionation and purification of the samples

M. citrifolia fruits (ripe and frozen), leaves, roots, and branches were collected in Okinawa Prefecture, Japan. Methanol extracts of each of these components of *M. citrifolia* were prepared and subjected to purification procedures, as described previously (15–18). In brief, the plant components were dried at room temperature, pulverized according to their characteristics, and then extracted with methanol at 50 °C for 6 hr. The extracts were then filtered and the filtrates concentrated by using an evaporator at temperatures not exceeding 40 °C. The residues thus obtained were resuspended in water and successively partitioned between *n*-hexane, ethyl acetate, and 1-butanol. Next, the *n*-hexane extracts were subjected to recycling preparative HPLC (solvent system, 100% methanol; column, GS-320; ID, 21.5 mm × 500 mm; flow rate, 5.0 mL/min; detection, UV 210 nm) to yield five fractions (Fr. 1–5). Fr. 5 was subjected to HPLC separation (solvent system, 100% methanol; column, TSK-gel GOLIGOPW [Tosoh Bioscience Diagnostics, Tessenderlo, Belgium]; ID, 4.6 mm × 250 mm; flow rate, 1.0 mL/min; detection, UV 210 nm) to yield three fractions (Fr. 5-1 to 5-3). Fr. 5-1 was rechromatographed by ODS column chromatography (Varian Mega Bond-Elut C18; Agilent Technologies Japan, Tokyo, Japan) with 100% methanol as an eluent to yield three fractions (Fr. 5-1-1 to 5-1-3). Fr. 5-1-3 was subjected to HPLC (solvent system, methanol–acetone [9:1]; column, Cosmosil Cholester [Nacalai Tesque, Kyoto, Japan]; ID, 4.6 mm × 450 mm; flow rate, 2 mL/min; detection, UV 400 nm) to obtain two fractions (Fr. 5-1-3-1 and 5-1-3-2).

The ^{1}H-NMR spectra were measured with a JEOL ECA 500 spectrometer (500 MHz; Tokyo, Japan). HPLC was performed on a JASCO LC-2000 plus system (JASCO, Tokyo, Japan). A Merck TLC plate (Art. 5715; Merck, Darmstadt, Germany) was used for TLC comparisons.

Chemicals

Chlorophyll a (from spinach) and sodium copper chlorophyllin were purchased from Sigma–Aldrich (St Louis, MO, USA) and pheophytin a from Wako Pure Chemical Industries (Osaka, Japan). Pheophorbide a and pyropheophorbide a were purchased from Frontier Scientific (Logan, UT, USA).

Analysis of anti-HCV activities of plant extracts and purified compounds

For anti-HCV activity assay, test samples were weighed and dissolved in DMSO to obtain stock solutions, which were stored at −20 °C until used. Huh7.5 cells were

seeded in 24-well plates (1.9×10^5 cells/well). A fixed amount of HCV was mixed with serial dilutions of the plant extracts (100, 30, 10, 3, and 1 μg/mL) and inoculated into the cells. After 2 hr, the cells were washed with medium to remove the residual virus and further incubated in medium containing the same concentrations of the plant extracts as those used during virus inoculation. In order to assess the mode of action of the samples examined, in some experiments treatment with the plant extracts was performed only during virus inoculation or only after virus inoculation until virus harvest. Culture supernatants were obtained at 1 and 2 days post-infection and titrated for virus infectivity, as described previously (19). Virus and cells treated with medium containing 0.1% DMSO served as controls. Percent inhibition of virus infectivity by the samples was calculated by comparing with the controls; IC_{50} were determined.

Time-of-addition experiments

To determine whether anti-HCV activities of the test samples occurred at the entry or the post-entry step, time-of-addition experiments were performed as described previously (6, 7). In brief:

1 HCV was mixed with each of the compounds and the mixture was inoculated into the cells. After virus adsorption for 2 hr, the residual virus and test sample were removed and the cells refed with fresh medium without the test sample for 46 hr. This experiment examines antiviral effect during the entry step.

2 HCV was inoculated into the cells in the absence of test samples. After virus adsorption for 2 hr, the residual virus was removed and the cells refed with fresh medium containing the test samples for 46 hr. This experiment examines the antiviral effect during the post-entry step.

3 As a positive control, HCV mixed with the test sample was inoculated into the cells. After virus adsorption for 2 hr, the residual virus and test sample were removed and the cells refed with fresh medium containing the test samples for 46 hr.

WST-1 assay for cytotoxicity

WST-1 assay was performed as described previously with a slight modification (19). In brief, Huh7.5 cells in 96-well plates were treated with serial dilutions of the plant extracts or 0.1% DMSO as a control for 48 hr. After this treatment, 10 μL of WST-1 reagent (Roche, Mannheim, Germany) was added to each well and the cells cultured for 4 hr. The WST-1 reagent is absorbed by the cells and converted to formazan by mitochondrial dehydrogenases. The amount of formazan, which correlates with the number of living cells, was determined by measuring the absorbance of each well using a microplate reader at 450 and 630 nm. Percent cell viability compared to the control was calculated for each dilution of the plant extracts and CC_{50} were determined.

Immunoblotting

Immunoblotting analysis was performed as described previously (6, 7, 20). In brief, cells lysed with an SDS sample buffer were subjected to SDS-PAGE and transferred onto polyvinylidene difluoride membranes (Millipore, Bedford, MA, USA). The membranes were incubated with the respective primary antibody, such as mouse monoclonal antibodies against HCV NS3 and GAPDH (Millipore). Horseradish peroxidase-conjugated goat anti-mouse immunoglobulin (Invitrogen) was used to visualize the respective proteins by means of an enhanced chemiluminescence detection system (GE Healthcare, Buckinghamshire, UK).

Real-time quantitative RT-PCR

Real-time quantitative RT-PCR was performed as described previously (6, 7, 20). In brief, 1 μg of total RNA extracted from the cells using a ReliaPrep RNA cell miniprep system (Promega, Madison, WI, USA) was reverse transcribed using a GoScript Reverse Transcription system (Promega) with random primers. The resultant cDNA was subjected to real-time quantitative PCR analysis using SYBR Premix Ex Taq (TaKaRa, Kyoto, Japan) in a MicroAmp 96-well reaction plate and an ABI PRISM 7500 system (Applied Biosystems, Foster City, CA, USA). The HCV NS5A-specific primers used were 5′-AGACGTATTGAGGTCCATGC-3′ (sense) and 5′-CCGCAGCGACGGTGCTGATAG-3′ (antisense). Human GAPDH gene expression measured by using primers 5′-GCCATCAATGACCCCTTCATT-3′ (sense) and 5′-TCTCGCTCCTGGAAGATGG-3′ (antisense) served as internal controls.

Statistical analysis

Results are expressed as mean ± SEM. Statistical significance was evaluated by Student's *t*-test. $P < 0.05$ was considered statistically significant.

RESULTS

Anti-HCV activities of methanol extracts of *M. citrifolia* fruits, leaves, roots, and branches

Methanol extracts of the fruits (ripe and frozen), leaves, roots, and branches of *M. citrifolia* were examined for antiviral activities against the HCV J6/JFH1-P47 strain.

It was found that a methanol extract of *M. citrifolia* leaves at a concentration of 30 μg/mL inhibits HCV infection by 98.3%, whereas extracts of ripe fruits, frozen fruits, roots and branches at the same concentration inhibit HCV infection by 23.4%, 34.0%, 59.6%, and 27.7%, respectively. The following analyses, therefore, focus on the extract from *M. citrifolia* leaves.

Anti-HCV activities of further purified samples of *M. citrifolia* leaves

The methanol extract of *M. citrifolia* leaves was further partitioned with different solvents, comprising *n*-hexane, ethyl acetate, 1-butanol and water, and their IC_{50}, CC_{50}, and SIs (SI: CC_{50}/IC_{50}) determined. The IC_{50} values of the partitions with *n*-hexane and ethyl acetate were 6.1 and 6.6 μg/mL, respectively; both of these showed stronger anti-HCV activities than did the methanol extract, which had an IC_{50} of 20.6 μg/mL (Table 1). The *n*-hexane-partitioned sample was fractionated into a further five fractions by a recycling preparative HPLC method; of these fractions, only Fr. 5 showed anti-HCV activity, the IC_{50} being 7.8 μg/mL (Table 2). Fr. 5 was therefore further purified by HPLC, ODS column chromatography and another HPLC and Fr. 5-1-3-2 identified as the most potent and purified fraction, having an IC_{50} of 4.6 μg/mL.

On TLC analysis (detection: UV irradiation 366 nm) of Fr. 5-1-3-2, a red-fluorescent spot was detected, suggesting that Fr. 5-1-3-2 consists almost solely of chlorophyll a and its degraded products. The presence of pheophorbide a, which is reportedly the major catabolite of chlorophyll a (21, 22), was confirmed by direct comparison with a standard sample by TLC analysis. Structural analyses using HPLC and NMR identified the purified compound as pheophorbide a (23).

Anti-HCV activities of pheophorbide a and pyropheophorbide a

Pheophorbide a is a breakdown product of chlorophyll. In its breakdown process, chlorophyll loses the Mg^{2+} ion through demetallation to generate pheophytin a in senescent leaves (21, 22). Pheophytin a is catabolized to pheophorbide a through dephytylation. In fruits, dephytylation of chlorophyll takes place first to generate chlorophyllide, which is then catabolized to pheophorbide a through demetallation. Pheophorbide a is further catabolized to generate pyropheophorbide a. On the other hand, sodium copper chlorophyllin is a semi-synthetic compound in which the Cu^{2+} ion replaces the Mg^{2+} ion.

Anti-HCV activities of commercially available, reagent-grade chlorophyll a and its-related compounds were examined. It was found that chlorophyll a barely, and sodium copper chlorophyllin and pheophytin a only weakly, exhibit anti-HCV activities (IC_{50} = 220, 32.0, and 54.5 μg/mL, respectively). On the other hand, pheophorbide a and pyropheophorbide a showed potent anti-HCV activities with IC_{50} of 0.3 and 0.2 μg/mL, respectively (Table 3).

Table 1. Anti-HCV activity (IC_{50}), cytotoxicity (CC_{50}) and selectivity index (SI) of a methanol extract and solvent partitions obtained from of *M. citrifolia* leaves

Sample	IC_{50} (μg/mL)	CC_{50} (μg/mL)	SI
Methanol extract	20.6	>30‡	>1.5
n-Hexane partition	6.1	>30‡	>4.9
Ethyl acetate partition	6.6	>30‡	>4.5
n-Butanol partition	20.8	>30‡	>1.5
Water partition	>30†	>30‡	na

†no detectable HCV inhibition at 30 μg/mL. ‡no detectable cytotoxicity at 30 μg/mL; na, not applicable.

Table 2. Anti-HCV activity (IC_{50}), cytotoxicity (CC_{50}), and selectivity index (SI) of fractions from *M. citrifolia* leaves obtained by recycling preparative HPLC and ODS column chromatography

Sample	IC_{50} (μg/mL)	CC_{50} (μg/mL)	SI
Fr. 1	>30	>30‡	na
Fr. 2	>30	>30‡	na
Fr. 3	>30†	>30‡	na
Fr. 4	>30†	>30‡	na
Fr. 5	7.8	>30‡	>3.8
ODS column chromatography			
Fr. 5-1-1	8.6	>30‡	>3.5
Fr. 5-1-2	5.2	>30‡	>5.8
Fr. 5-1-3	4.6	>30‡	>6.5
HPLC			
Fr. 5-1-3-1	>30	>30	na
Fr. 5-1-3-2	4.6	>30	>6.5

†no detectable HCV inhibition at 30 μg/mL. ‡no detectable cytotoxicity at 30 μg/mL; na, not applicable.

Table 3. Anti-HCV activity (IC_{50}), cytotoxicity (CC_{50}), and selectivity index (SI) of commercially available chlorophyll a, sodium copper chlorophyllin, pheophytin a, pheophorbide a, and pyropheophorbide a

Sample	IC_{50} (μg/mL)	CC_{50} (μg/mL)	SI
Chlorophyll a	220	>300	na
Sodium copper chlorophyllin	32.0	158	4.9
Pheophytin a	54.5	328	6.0
Pheophorbide a	0.3	10.0	33
Pyropheoborbide a	0.2	7.2	36

na, not applicable.

Table 4. Time-of-addition analysis of pheophorbide a and pyropheophorbide a against HCV

Compound (μg/mL)	Anti-HCV activity†		
	During virus inoculation	After virus inoculation	During & after virus inoculation
Pheophorbide a (1.0)	64.0	95.3	98.7
Pyropheophorbide a (0.5)	53.0	98.1	99.7

†% inhibition when tested by time-of-addition analysis.

Mode-of-action of pheophorbide a and pyropheophorbide a

To determine whether the anti-HCV effects of pheophorbide a and pyropheophorbide a are exerted during the entry or post-entry step, time-of-addition experiments were performed. It was found that, when added to the culture only during virus adsorption followed by virus entry, pheophorbide a (1.0 μg/mL) and pyropheophorbide a (0.5 μg/mL) inhibit HCV infection by 64.0% and 53.0%, respectively (Table 4). On the other hand, when added to the culture only after virus inoculation, they inhibited HCV replication by 95.3% and 98.1%, respectively. These results suggest that pheophorbide a and pyropheophorbide a act during both the entry and post-entry steps.

Inhibition of HCV RNA replication and HCV protein synthesis by pheophorbide a and pyropheophorbide a

To further confirm that pheophorbide a and pyropheophorbide a exert their anti-HCV activities not only during the virus entry step but also during the post-entry step (after the virus has entered the cells), Huh7.5 cells were inoculated with HCV for 2 hr in the absence of the test samples, and then treated with either one of the compounds for 1–2 days. Real-time quantitative RT-PCR and immunoblotting analyses demonstrated that both pheophorbide a and pyropheophorbide a inhibit HCV RNA replication in a dose-dependent manner (Fig. 1a) and, consequently, inhibit HCV protein synthesis in the cells (Fig. 1b).

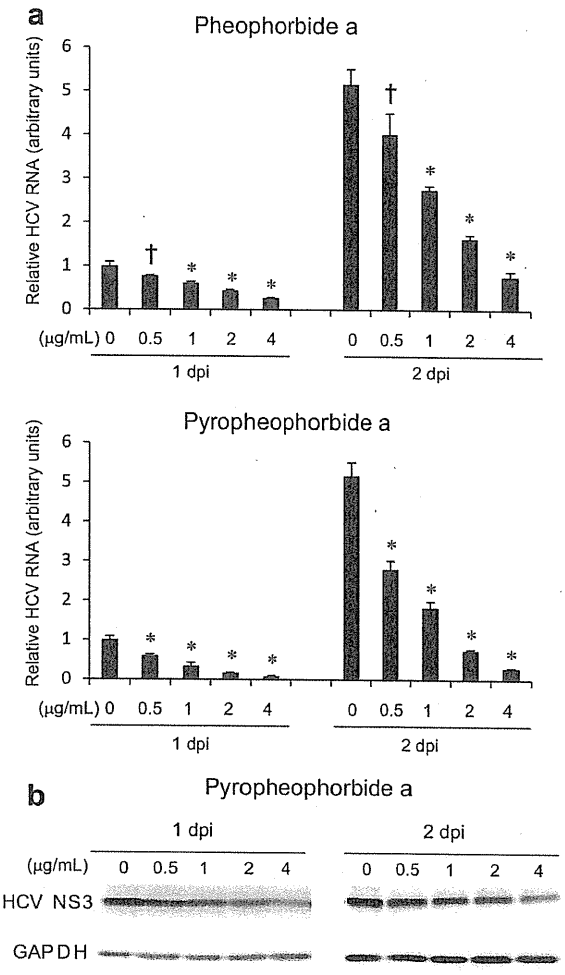

Fig. 1. Effects of pheophorbide a and pyropheophorbide a on HCV RNA replication and protein synthesis. (a) Huh 7.5 cells were inoculated with HCV J6/JFH1 at an MOI of 2.0. After 2 hr, the cells were washed with medium to remove residual virus and treated with either pheophorbide a or pyropheophorbide a (both at 0.5, 1.0, 2.0, and 4 μg/mL) or left untreated, and then subjected to real-time quantitative RT-PCR analysis 1 and 2 dpi. The HCV RNA amounts in the cells are normalized to degree of GAPDH mRNA expression. Data represent means ± SEMs of data from two independent experiments. The value for the untreated control at 1 dpi is arbitrarily expressed as 1.0. *, $P < 0.0001$. (b) Amounts of the HCV NS3 protein in the pyropheophorbide a-treated cells described in (a) were measured by western blot analysis using monoclonal antibody against the NS3 protein. GAPDH served as an internal control to verify equal amounts of sample loading.

DISCUSSION

It has been reported that methanol and ethanol extracts of *M. citrifolia* fruits show anti-HCV activities in a HCV subgenomic replicon system (12). In the present study, we found that a methanol extract of *M. citrifolia* leaves inhibits HCV replication in an HCV cell culture system more efficiently than do *M. citrifolia* fruits extracts (98% vs. ca. 30% inhibition at 30 μg/mL), the IC_{50} of the *M. citrifolia* leaves extract being 20.6 μg/mL (Table 1). Subsequent bioactivity-guided purification and structural analysis demonstrated that pheophorbide a, known to be the major catabolite of chlorophyll a (21, 22), and

its related catabolite, pyropheophorbide a, have potent anti-HCV activities (Table 3). A time-of-addition study suggested that pheophorbide a and pyropheophorbide a act during both the entry and post-entry steps (Table 4). It should be noted that, although Fr. 5-1-3-2 purified from the *M. citrifolia* leaves extract consists almost entirely of pheophorbide a, its anti-HCV activity is much weaker than that of reagent-grade pheophorbide a (Tables 2, 3). One possible explanation for this apparent discrepancy is that a copurified small molecule(s) in the fraction interfered with the anti-HCV activity of pheophorbide a. Further studies are needed to clarify this issue.

Pheophorbide a reportedly inhibits influenza A virus infection (24). Pheophorbide a and pyropheophorbide a also reportedly show antiviral activities against herpes simplex virus type 2 and influenza A virus, but not poliovirus (25). Given that herpes simplex virus type 2 and influenza A virus are envelope viruses whereas poliovirus is a non-envelope virus, Bouslama *et al.* speculate that pheophorbide a and pyropheophorbide a inhibit envelope viruses, targeting specific envelope proteins and thereby interfering with viral binding to the host cell receptors (25). On the other hand, our present results suggest that pheophorbide a and pyropheophorbide a inhibit HCV infection not only during the viral binding/entry step but also during the post-entry step (Table 4, Fig. 1). The post-entry step can be further divided into the following stages of the HCV lifecycle: (i) uncoating of the viral particles and capsid; (ii) synthesis and processing of the viral proteins and replication of the viral genome; and (iii) assembly, intracellular transport, and release of the viral particles (1, 26, 27). Now that we have shown that pheophorbide a and pyropheophorbide a inhibit HCV infection during the post-entry step, it is important to elucidate the specific molecular mechanism(s) in the viral lifecycle targeted by those compounds.

Pheophorbide a and pyropheophorbide a are known to induce photosensitivity: the resultant photo-activated characteristics play important anti-tumor roles in photodynamic therapy using pheophorbide a and its derivatives (28–30). Pheophorbide a also reportedly induces apoptosis of cancer cells and potentiates immunostimulating functions of macrophages (31, 32). However, photosensitivity can cause serious adverse effects when these agents are used to treat cancer and viral infections. Importantly, the photosensitizing effect can be separated from anti-tumor effect (28). It is therefore tempting to speculate that a new derivative(s) with more potent anti-HCV activities and less capacity to induce photosensitivity could be synthesized from the seed compounds of pheophorbide a and pyropheophorbide a.

It has previously been reported that pheophytin a shows anti-HCV activities with IC_{50} of 4.97 μM (equivalent to 4.3 μg/mL) (33). Also chlorophyllin, a semi-synthetic derivative of chlorophyll, reportedly has antiviral activities against poliovirus and bovine herpesvirus, with IC_{50} of 19.8 and 8.6 μg/mL, respectively (34). However, in our study, compared with the more potent anti-HCV activities of pheophorbide a and pyropheophorbide a, pheophytin a and sodium copper chlorophyllin exhibited only marginal anti-HCV activity, the IC_{50} being 54.5 and 32.0 μg/mL, respectively (Table 3).

In this study, we demonstrated anti-HCV activities of pheophorbide a and pyropheophorbide a using the J6/JFH1 strain of HCV genotype 2a (13, 14). Whether these compounds inhibit replication of other HCV strains of different genotypes is an important question to answer. Currently, some other HCV genotypes, such as genotypes 1a, 1b and 3a to 7a, are available for drug screening tests (2, 35). Such *in vitro* cell culture systems would help in determining the possible anti-HCV activities of pheophorbide a and pyropheophorbide a against different genotypes of HCV.

In conclusion, we have demonstrated that a methanol extract of *M. citrifolia* leaves and certain chlorophyll-derived compounds, such as pheophorbide a and pyropheophorbide a, possess anti-HCV activities. These compounds would be good candidates for seed compounds for developing novel antivirals against HCV.

ACKNOWLEDGMENTS

The authors are grateful to Dr. C.M. Rice (Rockefeller University, New York, NY, USA) for providing Huh-7.5 cells and pFL-J6/JFH1. This study was supported in part by Science and Technology Research Partnerships for Sustainable Development from JST and JICA. It was also performed as part of Japan Initiative for Global Research Network on Infectious Diseases (J-GRID), Ministry of Education, Culture, Sports, Science and Technology, Japan.

DISCLOSURE

The authors have no conflicts of interest to declare.

REFERENCES

1. Moradpour D., Penin F., Rice C.M. (2007) Replication of hepatitis C virus. *Nat Rev Microbiol* **5**: 453–6.
2. Gottwein J.M., Scheel T.K., Jensen T.B., Lademann J.B., Prentoe J.C., Knudsen M.L., Hoegh A.M., Bukh J., Development and characterization of hepatitis C virus genotype 1-7 cell culture systems: role of CD81 and scavenger receptor class B type I and effect of antiviral drugs. *Hepatology* **49** 2009; 364–77.

3. Shepard C.W., Finelli L., Alter M.J. (2005) Global epidemiology of hepatitis C virus infections. *Lancet Infect Dis* **5**: 558–67.
4. Arzumanyan A., Reis H.M., Feitelson M.A. (2013) Pathogenic mechanisms in HBV- and HCV-associated hepatocellular carcinoma. *Nat Rev Cancer* **13**: 123–35.
5. Calland N., Dubuisson J., Rouille Y., Seron K. (2012) Hepatitis C virus and natural compounds: a new antiviral approach?. *Viruses* **4**: 2197–217.
6. Wahyuni T.S., Tumewu L., Permanasari A.A., Apriani E., Adianti M., Rahman A., Widyawaruyanti A., Lusida M.I., Fuad A., Soetjipto D., Nasronudin D., Fuchino H., Kawahara N., Shoji I., Deng L., Aoki C., Hotta H. (2013) Antiviral activities of Indonesian medicinal plants in the East Java region against hepatitis C virus. *Virol J* **10**: 259.
7. Adianti M., Aoki C., Komoto M., Deng L., Shoji I., Wahyuni T.S., Lucida M.I., Soetjipto, Fuchino H., Kawahara N., Hotta H. (2014) Anti-hepatitis C virus compounds obtained from *Glycyrrhiza uralensis* and other *Glycyrrhiza* species. *Microbiol Immunol*. doi: 10.1111/1348-0421.12127. [Epub ahead of print].
8. Ikuta K., Hashimoto K., Kaneko H., Mori S., Ohashi K., Suzutani T. (2012) Anti-viral and anti-bacterial activities of an extract of blackcurrants (*Ribes nigrum L.*). *Microbiol Immunol* **56**: 805–9.
9. Serafini M.R., Santos R.C., Guimarães A.G., Dos Santos J.P., da Conceicão Santos A.D., Alves I.A., Gelain D.P., de Lima Nogueira P.C., Quintans-Júnior L.J., Bonjardim L.R., de Souza Araújo A.A. (2011) *Morinda citrifolia* Linn leaf extract possesses antioxidant activities and reduces nociceptive behavior and leukocyte migration. *J Med Food* **14**: 1159–66.
10. Nakanishi K., Sasaki S., Kiang A.K., Goh J., Kakisawa H., Ohashi M., Goto M., Watanabe J., Yokotani H., Matsumura C., Togashi M. (1965) Phytochemical survey of Malaysian plants preliminary chemical and pharmacological screening. *Chem Pharm Bull* **13**: 882–90.
11. Saludes J.P., Garson M.J., Franzblau S.G., Aguinaldo A.M. (2002) Antitubercular constituents from the hexane fraction of *Morinda citrifolia* Linn. (Rubiaceae). *Phytother Res* **16**: 683–5.
12. Selvam P., Murugesh N., Witvrouw M., Keyaerts E., Neyts J. (2009) Studies of antiviral activity and cytotoxicity of *Wrightia tinctoria* and *Morinda citrifolia*. *Indian J Pharm Sci* **71**: 670–2.
13. Lindenbach B.D., Evans M.J., Syder A.J., Wolk B., Tellinghuisen T.L., Liu C.C., Maruyama T., Hynes R.O., Burton D.R., McKeating J.A., Rice C.M. (2005) Complete replication of hepatitis C virus in cell culture. *Science* **309**: 623–6.
14. Bungyoku Y., Shoji I., Makine T., Adachi T., Hayashida K., Nagano-Fujii M., Ide Y., Deng L., Hotta H. (2009) Efficient production of infectious hepatitis C virus with adaptive mutations in cultured hepatoma cells. *J Gen Virol* **90**: 1681–91.
15. Li S.Y., Fuchino H., Kawahara N., Sekita S., Satake M. (2002) New phenolic constituents from *Smilax bracteata*. *J Nat Prod* **65**: 262–6.
16. Fuchino H., Sekita S., Mori M., Kawahara N., Satake M., Kiuchi F. (2008) A new leishmanicidal saponin from *Brunfelsia grandiflora*. *Chem Pharm Bull* **56**: 93–6.
17. Fuchino H., Kawano M., Mori-Yasumoto K., Sekita S., Satake M., Ishikawa T., Kiuchi F., Kawahara N. (2010) *In vitro* leishmanicidal activity of benzophenanthridine alkaloids from *Bocconia pearcei* and related compounds. *Chem Pharm Bull* **58**: 1047–50.
18. Fuchino H., Daikonya A., Kumagai T., Goda Y., Takahashi Y., Kawahara N. (2013) Two new labdane diterpenes from fresh leaves of Leonurus japonicas and their degradation during drying. *Chem Pharm Bull* **61**: 497–503.
19. Deng L., Adachi T., Kitayama K., Bungyoku Y., Kitazawa S., Ishido S., Shoji I., Hotta H. (2008) Hepatitis C virus infection induces apoptosis through a Bax-triggered, mitochondrion-mediated, caspase 3-dependent pathway. *J Virol* **82**: 10375–85.
20. Deng L., Shoji I., Ogawa W., Kaneda S., Soga T., Jiang D.P., Ide Y.H., Hotta H. (2011) Hepatitis C virus infection promotes hepatic gluconeogenesis through an NS5A-mediated, FoxO1-dependent pathway. *J Virol* **85**: 8556–68.
21. Hörtensteiner S., Kräutler B. (2011) Chlorophyll breakdown in higher plants. *Biochim Biophys Acta* **1807**: 977–88.
22. Hörtensteiner S. (2013) Update on the biochemistry of chlorophyll breakdown. *Plant Mol Biol* **82**: 505–17.
23. Cheng H.H., Wang H.K., Ito J., Bastow K.F., Tachibana Y., Nakanishi Y., Xu Z., Luo T.Y., Lee K.H. (2001) Cytotoxic pheophorbide-related compounds from *Clerodendrum calamitosum* and *C. cyrtophyllum*. *J Nat Prod* **64**: 915–9.
24. Yasuda T., Yamaki M., Iimura A., Shimotai Y., Shimizu K., Noshita T., Funayama S. (2010) Anti-influenza virus principles from *Muehlenbeckia hastulata*. *J Nat Med* **64**: 206–11.
25. Bouslama L., Hayashi K., Lee J.B., Ghorbel A., Hayashi T. (2011) Potent virucidal effect of pheophorbide a and pyropheophorbide a on enveloped viruses. *J Nat Med* **65**: 229–33.
26. Ploss A., Dubuisson J. (2012) New advances in the molecular biology of hepatitis C virus infection: towards the identification of new treatment targets. *Gut* **61** (Suppl 1): i25–35.
27. Aly H.H., Shimotohno K., Hijikata M., Seya T. (2012) In vitro models for analysis of the hepatitis C virus life cycle. *Microbiol Immunol* **56**: 1–9.
28. Nakamura Y., Murakami A., Koshimizu K., Ohigashi H. (1996) Identification of pheophorbide a and its related compounds as possible anti-tumor promoters in the leaves of *Neptunia oleracea*. *Biosci Biotechnol Biochem* **60**: 1028–30.
29. Gil M., Bieniasz M., Seshadri M., Fisher D., Ciesielski M.J., Chen Y., Pandey R.K., Kozbor D. (2011) Photodynamic therapy augments the efficacy of oncolytic vaccinia virus against primary and metastatic tumours in mice. *Br J Cancer* **105**: 1512–21.
30. Rapozzi V., Zorzet S., Zacchigna M., Drioli S., Xodo L.E. (2013) The PDT activity of free and pegylated pheophorbide a against an amelanotic melanoma transplanted in C57/BL6 mice. *Invest New Drugs* **31**: 192–9.
31. Bui-Xuan N.H., Tang P.M., Wong C.K., Fung K.P. (2010) Photo-activated pheophorbide-a, an active component of *Scutellaria barbata*, enhances apoptosis via the suppression of ERK-mediated autophagy in the estrogen receptor-negative human breast adenocarcinoma cells MDA-MB-231. *J Ethnopharmacol* **131**: 95–103.
32. Bui-Xuan N.H., Tang P.M., Wong C.K., Chan J.Y., Cheung K.K., Jiang J.L., Fung K.P. (2011) Pheophorbide a: a photosensitizer with immunostimulating activities on mouse macrophage RAW 264. 7 cells in the absence of irradiation. *Cell Immunol* **269**: 60–7.
33. Wang S.Y., Tseng C.P., Tsai K.C., Lin C.F., Wen C.Y., Tsay H.S., Sakamoto N., Tseng C.H., Cheng J.C. (2009) Bioactivity-guided screening identifies pheophytin a as a potent anti-hepatitis C virus compound from *Lonicera hypoglauca* Miq. *Biochem Biophys Res Commun* **385**: 230–5.
34. Benati F.J., Lauretti F., Faccin L.C., Nodari B., Ferri D.V., Mantovani M.S., Linhares R.E., Nozawa C. (2009) Effects of chlorophyllin on replication of poliovirus and bovine herpesvirus in vitro. *Lett Appl Microbiol* **49**: 791–5.
35. Date T., Morikawa K., Tanaka Y., Tanaka-Kaneko K., Sata T., Mizokami M., Wakita T. (2012) Replication and infectivity of a novel genotype 1b hepatitis C virus clone. *Microbiol Immunol* **56**: 308–17.

Microbiology and Immunology

Microbiol Immunol 2014; 58: 180–187
doi: 10.1111/1348-0421.12127

ORIGINAL ARTICLE

Anti-hepatitis C virus compounds obtained from *Glycyrrhiza uralensis* and other *Glycyrrhiza* species

Myrna Adianti[1,2], Chie Aoki[1,3], Mari Komoto[1], Lin Deng[1], Ikuo Shoji[1], Tutik Sri Wahyuni[1,2], Maria Inge Lusida[2], Soetjipto[2], Hiroyuki Fuchino[4], Nobuo Kawahara[4] and Hak Hotta[1]

[1]Division of Microbiology, Kobe University Graduate School of Medicine, 7-5-1 Kusunoki-cho, Chuo-ku, Kobe 650-0017, [2]Institute of Tropical Disease, Airlangga University, Jl. Mulyorejo, Surabaya 60115, [3]Japan Science and Technology/Japan International Cooperation Agency Science and Technology Research Partnership for Sustainable Development Laboratory (JST/JICA SATREPS), Faculty of Medicine, University of Indonesia, Jl. Salemba 4, Jakarta 10430, Indonesia and [4]Research Center for Medicinal Plant Resources, National Institute of Biomedical Innovation, 1–2, Hachimandai, Tsukuba City, Ibaraki Prefecture 305-0843, Japan

ABSTRACT

Development of complementary and/or alternative drugs for treatment of hepatitis C virus (HCV) infection is still much needed from clinical and economic points of view. Antiviral substances obtained from medicinal plants are potentially good targets to study. *Glycyrrhiza uralensis* and *G. glabra* have been commonly used in both traditional and modern medicine. In this study, extracts of *G. uralensis* roots and their components were examined for anti-HCV activity using an HCV cell culture system. It was found that a methanol extract of *G. uralensis* roots and its chloroform fraction possess anti-HCV activity with 50%-inhibitory concentrations (IC_{50}) of 20.0 and 8.0 μg/mL, respectively. Through bioactivity-guided purification and structural analysis, glycycoumarin, glycyrin, glycyrol and liquiritigenin were isolated and identified as anti-HCV compounds, their IC_{50} being 8.8, 7.2, 4.6 and 16.4 μg/mL, respectively. However, glycyrrhizin, the major constituent of *G. uralensis*, and its monoammonium salt, showed only marginal anti-HCV activity. It was also found that licochalcone A and glabridin, known to be exclusive constituents of *G. inflata* and *G. glabra*, respectively, did have anti-HCV activity, their IC_{50} being 2.5 and 6.2 μg/mL, respectively. Another chalcone, isoliquiritigenin, also showed anti-HCV activity, with an IC_{50} of 3.7 μg/mL. Time-of-addition analysis revealed that all *Glycyrrhiza*-derived anti-HCV compounds tested in this study act at the post-entry step. In conclusion, the present results suggest that glycycoumarin, glycyrin, glycyrol and liquiritigenin isolated from *G. uralensis*, as well as isoliquiritigenin, licochalcone A and glabridin, would be good candidates for seed compounds to develop antivirals against HCV.

Key words antiviral substance, coumarin, *Glycyrrhiza uralensis*, hepatitis C virus.

Hepatitis C virus is a member of the genus *Hepacivirus* and the family *Flaviviridae*. Based on the heterogeneity of the viral genome, HCV is currently classified into seven genotypes (1–7) and more than 67 subtypes (1a, 1b, 2a, 2b etc.) (1, 2). The viral genome, a single-stranded, positive-sense RNA of 9.6 kb, encodes a polyprotein precursor consisting of about 3000 amino acid residues that is cleaved by host and viral proteases to generate 10 mature proteins, namely core, E1, E2, a putative ion channel p7, and nonstructural proteins NS2, NS3, NS4A, NS4B, NS5A and NS5B (3). Core, E1 and E2 are components of the infectious virus particle together

Correspondence
Hak Hotta, Division of Microbiology, Kobe University Graduate School of Medicine, 7-5-1 Kusunoki-cho, Chuo-ku, Kobe, 650-0017, Japan.
Tel: +81 78 382 5500; fax: +81 78 382 5519. email: hotta@kobe-u.ac.jp

Received 4 December 2013; revised 20 December 2013; accepted 25 December 2013.

List of Abbreviations: CC_{50}, 50%-cytotoxic concentrations; E, envelope; Fr, fraction; GAPDH, glyceraldehyde-3-phosphate dehydrogenase; HCV, hepatitis C virus; IC_{50}, 50%-inhibitory concentration; ID, internal diameter; SI, selectivity index.

with the viral genome; however, the nonstructural proteins constitute the viral replication complex, where replication of the viral genome takes place. The HCV proteins also play essential roles in the pathological processes associated with HCV infection, such as carcinogenesis and glucose and lipid metabolic disorders (4, 5).

Hepatitis C virus is among the major causative agents of chronic hepatitis, hepatic cirrhosis and hepatocellular carcinoma (5–7). The global prevalence of HCV is >2.5%; thus, about 180 million people are chronically infected with this virus worldwide. A variety of standard treatment regimens using combinations of pegylated interferon, ribavirin and other direct-acting agents, such as HCV-specific inhibitors against NS3 protease and NS5A, have been adopted with considerable success. However, some clinically important issues remain unsolved, such as the emergence of drug-resistant virus and the cost of these drugs. Therefore, development of complementary and/or alternative drugs, especially those from medicinal plants, for treating HCV infection is still much needed from both clinical and economic points of view (8, 9).

Glycyrrhiza uralensis and *G. glabra* have been widely used as supplementary treatments in both traditional herbal medicine and modern medicine (10, 11). The radix of *Glycyrrhiza* spp. is commonly known as "gan cao" in Chinese and licorice in English. Bioactive constituents of *Glycyrrhiza* species can be classified into triterpenoids (such as glycyrrhizic acid), coumarins (such as glycycoumarin, glycyrin and glycyrol), flavones (such as liquiritin and liquiritigenin), chalcones (such as isoliquiritigenin and licochalcone A), isoflavans (such as glabridin), stilbenoids and other miscellaneous compounds (11). Glycyrrhizic acid, also known as glycyrrhizin and considered the principal component of *Glycyrrhiza* spp., is a glycosylated triterpenoid saponin that consists of one molecule of glycyrrhetinic acid and two molecules of D-glucuronic acid. Upon hydrolysis, the aglycone, 18β-glycyrrhetinic acid (simply called glycyrrhetinic acid), and two molecules of D-glucuronic acid are released. Glycyrrhizin and other compounds isolated from *Glycyrrhiza* species reportedly have antiviral activity against a variety of viruses, including HIV, herpes simplex virus, influenza virus, severe acute respiratory syndrome coronavirus, hepatitis viruses and enteroviruses (11–15). As for hepatitis viruses, glycyrrhizin has been used to treat liver diseases, including chronic hepatitis B and C (10). Although glycyrrhizin decreases serum alanine aminotransferase concentrations in HCV-infected patients, it does not significantly reduce amounts of HCV RNA (16, 17). It has been reported that a glycyrrhizin-containing preparation reduces hepatic steatosis in transgenic mice expressing the full-length HCV polyprotein (18). Recently, anti-HCV activity of glycyrrhizin *in vitro* was reported (19, 20). However, clear evidence for it still appears to be lacking.

In this study, we used an HCV cell culture system to examine a methanol extract and a chloroform subfraction of *G. uralensis* and certain isolated compounds, as well as commercially available purified compounds, such as glycyrrhizin and glycyrrhetinic acid, for their anti-HCV activity. We report here that glycycoumarin, glycyrin, glycyrol and liquiritigenin isolated from *G. uralensis* showed anti-HCV activity whereas glycyrrhizin showed only a marginal anti-HCV activity. We also found that some other constituents of *G. uralensis* or of *G. inflata* and *G. glabra*, such as isoliquiritigenin, licochalcone A and glabridin, showed anti-HCV activity.

MATERIALS AND METHODS

Cells and viruses

Huh7.5 cells and the plasmid pFL-J6/JFH1 (21) were kindly provided by Dr. C. M. Rice (Rockefeller University, New York, NY, USA). Huh7.5 cells were cultured in Dulbecco's modified Eagle's medium supplemented with FBS (Biowest, Nuaillé, France), non-essential amino acids (Invitrogen, Carlsbad, CA, USA), penicillin (100 IU/mL) and streptomycin (100 μg/mL) (Invitrogen) at 37 °C in a 5% CO_2 incubator. A cell culture-adapted strain of HCV genotype 2a (J6/JFH1-P47) was prepared as described previously (22) and used in this study at an MOI of 2.0.

Extraction, sub-fractionation and purification of *G. uralensis* roots

G. uralensis roots were purchased from Tochimoto Tenkaido (Osaka, Japan). A methanol extract of G. uralensis roots was prepared and subjected to purification procedures, as described previously (23–26). In brief, *G. uralensis* roots were dried at room temperature and pulverized. They were then extracted with methanol at 50 °C for 6 hr. The extracts were filtered and the filtrates concentrated by using an evaporator at temperatures not exceeding 40 °C. The residues obtained were re-suspended in water and successively partitioned between chloroform and *n*-butanol. The chloroform extract was subjected to recycling preparative HPLC (solvent system, 100% methanol; column, GS-320 + GS-310, 21.5 mm ID × 1000 mm, flow rate; 5.0 mL/min; detection, UV 210 nm: Condition A) to afford 10 fractions (Fr.1 to Fr.10). Fr.7 was subjected to HPLC

separation (solvent system, acetonitrile–water; column, Imtakt Unison UK-C18C (Kyoto, Japan), 4.6 mm ID × 250 mm; flow rate, 2.0 mL/min; detection, UV 254 nm) to give 12 fractions (Fr.7–1 to 7–12) and glycyrin (2.5 mg; Fr.7–9). Fr.7–6 was purified by recycling HPLC (Condition A) to afford glycycoumarin (0.7 mg). Fr.8- to Fr.10 were combined and then re-chromatographed by HPLC (solvent system, acetonitrile–water; column, Imtakt Unison UK-C18C, 4.6 mm ID × 250 mm; flow rate, 2.0 mL/min; detection, UV 254 nm) to give 15 fractions (Fr.8–1 to Fr.8–15). Fr.8–3 was subjected to recycling HPLC (Condition A) to give liquiritigenin (1.2 mg). Fr.8–9 was purified by recycling HPLC (Condition A) to afford glycyrol (1.1 mg). The ^{1}H- and ^{13}C-NMR spectra were measured with a Jeol ECA 500 spectrometer (500 MHz; Tokyo, Japan). HPLC was performed on a JASCOLC-2000 plus system (Tokyo, Japan).

Chemicals

Glycyrrhizic acid (cat. no. 074-03481), glycyrrhizic acid mono-ammonium salt *n*-hydrate (cat. no. 075-02171), glycyrrhetinic acid (cat. no. 072-02181) and glabridin (cat. no. 070-04821) were purchased from Wako Pure Chemical Industries (Osaka, Japan). Liquiritin (cat. no. L8045), liquiritigenin (cat. no. 78825) and licochalcone A (cat. no. 68783) were purchased from Sigma–Aldrich (Tokyo, Japan) and isoliquiritigenin (cat. no. I0822) from Tokyo Chemical Industry (Tokyo, Japan). Licorice-saponins G2 (cat. no. P2502) and H2 (cat. no. P2503), and glycyrrhetic acid 3-*O*-glucuronide (cat. no. NH080502) were purchased from Funakoshi (Tokyo, Japan). Glycycoumarin, glycyrol, glycyrin and liquiritigenin were isolated from *G. uralensis* extracts in this study, as described above.

Analysis of anti-HCV activity of plant extracts and purified compounds

Test samples were weighed and dissolved in DMSO to obtain stock solutions at 10 or 30 mg/mL. The stock solutions were stored at −20 °C until used. Huh7.5 cells were seeded in 24-well plates (1.6×10^5 cells/well). HCV was mixed with serial dilutions of the test samples (100, 30, 10, 3 and 1 μg/mL) and inoculated into the cells. After 2 hr, the cells were washed with medium to remove residual virus and further incubated in medium containing the same concentrations of the samples as those during virus inoculation. In time-of-addition experiments, treatment with the samples was performed only during or after virus inoculation in order to assess the mode of action of the samples examined. Culture supernatants were collected 1 and 2 days post-infection and titrated for virus infectivity, as described below. Virus and cells treated with medium containing 0.1% DMSO served as controls. Percent inhibition of the virus infectivity for each dilution of the samples was calculated by comparison with mock-treated controls and IC_{50} determined.

Virus titration

Virus samples were diluted serially 10-fold in complete medium and inoculated onto Huh7.5 cells seeded on glass coverslips in a 24-well plate. After virus adsorption for 2 hr, the cells were washed with medium to remove residual virus and cultured for 24 hr. The virus-infected cells were stained with an indirect immunofluorescence method as reported previously (27). In brief, the virus-infected cells were washed with PBS, fixed with 4% paraformaldehyde for 15 min and permeabilized with 0.1% Triton X-100 in PBS for 15 min at room temperature. After being washed three times with PBS, the cells were incubated with HCV-infected patient's serum for 1 hr, followed by incubation with FITC-conjugated goat anti-human IgG (MBL, Nagoya, Japan). The cells were counterstained with Hoechst 33342 (Molecular Probes, Eugene, OR, USA) for 5 min and HCV-infected cells were counted under a BZ-9000 fluorescence microscope (Keyence, Osaka, Japan).

Cytotoxicity assay

The cytotoxicity of the samples was assessed by WST-1 assay as described previously with a slight modification (27). In brief, Huh7.5 cells in 96-well plates were treated with serial dilutions of the samples or 0.1% DMSO as a control for 48 hr. At the end of the treatment, 10 μL of WST-1 reagent (Roche, Mannheim, Germany) was added to each well and the cells cultured for 1 hr. The WST-1 reagent is absorbed by the cells and converted to formazan by mitochondrial dehydrogenases. The amount of formazan, which correlates with the number of living cells, was determined by measuring the absorbance of each well using a microplate reader at 450 and 630 nm. Percent cell viability compared to the control was calculated for each dilution of the samples and CC_{50} were determined.

Immunoblotting

Cells were lysed with an SDS sample buffer, after which equal amounts of protein were subjected to SDS–polyacrylamide gel electrophoresis and transferred onto a polyvinylidene difluoride membrane (Millipore, Bedford, MA, USA), as described previously (28, 29). The membranes were incubated with the respective primary